University Of Twente

Project Module 7

Project Fluid Engineering 2019-2020

Design and analysis of an in-flight anti-icing system for an airplane wing

Authors
T.W. Albers s2016273
J.L. Alvarez s2032147
S.A. Benítez s2074842
R.T.B. Bos s2189577
L.A Pérez s2029413
E.E Quimi s2029405
B.J. Schumer s2159473
J. Setz s2176971

Student Assistant
M. Heimgartner

Tutor
R. Hagmeijer

November 4, 2021

Preface

This report is written for the project of Fluid Mechanics and Heat Transfer 2019-2020 on the University of Twente.

For the assignment, an anti-icing system has to be designed for an airplane, which is a Boeing 737. Material presented by the courses and lecturers were primarily used. Furthermore, other reports and scientific articles presented on Canvas were used in order to understand the functions and backgrounds of multiple theorems and concepts. Additionally, several online sources were used, which are all mentioned in the references.

As a project group, we would like to thank all the lecturers for their lectures and working courses (Especially during the end). We would like to thank R. Hagmeijer and M. Heimgartner for their valuable input at the meetings and for answering most of our questions.

Abstract

On October 31, 1993, American Eagle Flight 4184 was on route from Indianapolis international Airport, Indiana, to O'Hare International Airport, Chicago. Bad weather during the day in Chicago caused many delays and this was prompting the air traffic control to hold Flight 4184 in holding in the nearby intersection at 10.000 ft. While holding, the plane came into a freezing rain, a dangerous icing condition where supercooled water droplets rapidly cause intense ice build-up. After this the Flight was ordered another two holds. During the descent, a sound in the cockpit, indicating an overspeed warning due to the extended flaps was heard in the cockpit. This is normally a moment for pilots for retracting the flaps, but after doing this a strange noise was heard on the cockpit voice recorder, followed by a sharp, uncommanded roll excursion that disengaged the autopilot. Later on, the flight recorder data showed that the aircraft subsequently went through at least one full roll, after the crew regained control of the rapidly descending aircraft. However, another roll occurred shortly after as they engaged the autopilot again. This second occurrence was unrecoverable, after that within less than thirty seconds, at 3.59 p.m., the contact with Flight 4184 was lost. This was because the plane had crashed nose-down into a soybean field near Roselawn, Indiana, killing all 64 passengers and 4 crew on board. After this crash there were some other crashes caused by ice accretion.

In order to prevent the icing with all its consequences from happening, aircrafts are equipped with a so called anti-icing system. In this project assignment, the main goal is to design an efficient anti-icing system, for the most critical situation of a specific aircraft, the Boeing 737.

Summary

This report had the objective of interconnect the subjects of heat transfer, fluid mechanics and apply the knowledge obtained through the module of study into the development of an organized research, analysis procedure and solution for a problem given which is the design of an anti-icing system for the wing of a certain type of aircraft, in this case a Boeing 737.

In the first part of the report a detailed research was elaborated in which necessary information regarding ice accretion definition and influence on aircraft is given, as well as existing systems which could be taken as a guide and as an opportunity for possible improvements, besides this, aviation certificates which set the limits of law when working on the design part and finally the problem definition.

After literature study part, the analysis could be started with external flows acting on an aircraft and on which for example trajectories and mass balances were calculated, with the help of 2DFOIL-ICE program ice accretion simulations could be done in a more detailed way and the worst case scenario for ice accretion had been set according to the literature study part in order to get values like which temperature and heat flux are needed to allow the de-icing of a wing when weather and aircraft conditions are the most dangerous regarding ice formation.

Once the external analysis was done, the internal flows were calculated for different types of heat transfer methods, like for example conduction, radiation, convection or mixed systems to proof efficiency and whether or not this systems would perform in a way that allows them to reach the necessary values for the de-icing of the wing. from this point a clue of which is systems are feasible to work is obtained.

With the previous information the design and optimization phase could be done in which a more detailed analysis of temperature distribution on the wing is made taking into account heating mats and impinging jets systems. An optimization for the impinging jets system is developed and it is also included the analysis of a possible application of ice-phobic materials.

At the end of this report a discussion and conclusions for the different parts of the report were included, in which a final system is chosen and the reasons are also stated.

Contents

Nomenclature

β	Coefficient of volume expansion [1/V] ($\beta = 1/T$ for ideal gases)
V	Volume[m^3]
δ	Velocity boundary layer [m]
$\dot{m}$	Mass flow [kg/s]
$\dot{Q}$	rate of heat transfer [J/s]
$\dot{q}$	heat flux [W/m^2]
μ	Viscosity [kg/ms]
ρ	Density [kg/m^3]
ρ_d	Density of droplet [kg/m^3]
ρ_a	Density of air [kg/m^3]
ρ_w	Density of water [kg/m^3]
ϕ	Velocity field [m/s]
U	Velocity [m/s]
u_w	Velocity of water [m/s]
C_D	Drag coefficient []
c_p	Specific heat at constant pressure [kJ/kgK]
E	Total energy [J]
H	Distance from impinging jets to nozzle [m]
H/d	Ration of distance from the nozzle and jet diameter []
H	Total enthalpy [J]
h	Specific enthalpy [J]
k	Thermal conductivity [W/mK]
σ	Stress [Pa]
p	Pressure [Pa]
θ	Angle [deg]or[rad]
ϵ	Emissivity []
As	Surface area [m^2]

Ac Cross-section area $[m^2]$

g Gravity acceleration $[m/s^2]$

Bi Biot number []

Gr Grashof number []

Re Reynolds number []

Re_d Reynolds number of droplet []

Nu Nusselt number []

Pr Prandtl number []

LWC Liquid water content $[kg/m^3]$

SLD Supercooled large droplets

SLW Supercooled liquid water

MED Mean effective diameter [m]

N_jet Number of impinging jets []

K Langmuir parameter []

T Temperature $[\deg C] or [K]$

t time [s]

Introduction

This report is made with the intention of designing an aircraft anti-icing system. Aircraft icing is defined as "flight in cloud in temperatures at or below freezing when supercooled water droplets impinge and freeze on the unprotected areas on which they impact" [1]. The two most harmful impacts that this has on the aerodynamic performance of the plane are: First, the change in form of the airfoil due to the ice will drastically increase the drag forces, increasing the forces of the turbines needed for flying. Second, also due to the change of shape of the airfoil the lift forces that keep the airplane in the air are reduced. Therefore a design of a good anti-icing system is really necessary for the safety of all the passengers on a Boeing 737-Max.

In order to design this anti-icing system, first the conditions at which it occurs need to be determined. For this reason a Literature Study has been done, with this some important parameters that need to be taken into account were found, including pressure altitude, droplet size, liquid water content of the droplets, temperature at which supper cooled droplets are formed, among other parameters. Another valuable information is the types of ice formation, for this, three are the most important: Rime-ice, Glaze-ice and Mixed-ice, and the different effects that have on the aerodynamic performance.

To come up with a suitable ant-icing system. First, four already existing designs are going to be analyzed: electric heating mats, radiation from a radiating object, forced convection and finally impinging jets. At the end, the performance of this designs are going to be compared, in order to choose the most suitable design as a starting point. Then, the corresponding optimizations are going to be made at this design, adjusting all the free variables for adapting this system to an airplane Boeing 737. Also the consideration of ice-phobic materials is going to be consider to make the system even more effective against the ice formation.

1 Literature study and problem definition

1.1 Ice accretion influence on aircraft aerodynamic performance

[1] defines aircraft icing as "flight in cloud in temperatures at or below freezing when supercooled water droplets impinge and freeze on the unprotected areas on which they impact". Ice have several impacts on the aerodynamics of an aircraft, some are very dangerous and can cause the aircraft to fail and crash, others are less critical but affect the efficiency of the airplane increasing the consumption of fuel which in turn increase the costs. In this part of the essay ice accretion is outlined, including: increase in drag forces, decrease in lift forces, pitch and roll upset phenomenon, and reduction in efficiency. Afterwards more detailed information about the ambient conditions where icing occurs and the different types of icing are going to be discuss.

Drag increase
Drag is a force generated when the solid surface of the aircraft and air (which is a fluid) move at different velocities, it is mainly caused by the disturbances of the air flow due to irregularities in the air-frame. Ice accretion acts as irregularities on the plane that increase the roughness of the surface mainly on the wings, therefore increasing the drag forces. This increment in drag force will come up with an increasing torque on the engine or transmission, in order to avoid a bad functioning of the plane pay special attention on this force [1].

Decrease lift
Another important aspect is the decrease in lift forces, that are caused by the change of shape of the airfoil due to ice accretion. Ice adders to the surfaces of the wing, this alters its shape creating a deficiency in the lifting forces that act on it. Vukits (2002) states that "the reduction in maximum lift equates to reduction in the stall angle of attack of the wing". This means that if the lift force decrease the critical angle of attack will also decrease, for this reason the speed of the plane has to be enough to counter the decrease in lift force, otherwise the angle of attack will be lower than its minimum permissible and the plane will go into loss. Therefore, higher speeds are required to maintain reasonable forces that keep the airplane in flight.

Pitch upset and Roll upset
Horizontal tail is after the wings the most important part of an aircraft, this acts as a counter moment (the wing aerodynamic moment). This is necessary to stabilise the plane. The thickness on the horizontal tail is usually smaller than in the wings, this causes a higher probability on ice accretion because the airflow is separated later than when a ticker airfoil does. When ice accretion occurs there can be two types, symmetric and asymmetric wing ice distribution.

If symmetric ice accretion is affecting the plane its consequences are more dangerous during the take-offs and landings, this is mainly because the speed is reduced and the flaps that control the angle of attack of the wing are increased also increasing the lift force on the wings generating a higher momentum that the horizontal tail will not able to counter due to the ice. Also, "the presence of ice on the tail also reduce the elevator effectiveness by 12 percent for the clean configuration, and by 16 percent with 10 degrees of flaps" (Vukits,2002), this phenomenon is called "pitch upset".

If asymmetric ice accretion acts on the wings, it means that the ice is not equally distributed in both wings (one wing has more ice accumulation than the other). This has a power full impact on the performance of the plane, something that is called "roll upset". When one of the wings present more ice it losses more lift force than the other creating a unbalance and making the plane to roll.

Reduction in efficiency
Another effect of ice accretion is the increase in weight, although this phenomenon has not a very high risk because this increment is very small and has not a high impact on the total weight of the plane, it has a influence on the efficiency. These multiple facts that reduce the performance of the aircraft create an efficiency problem. Due to the increase in drag force and decrease in lift force and increase in weight more energy is needed for the same performance in normal conditions. Thrust must be increased in order to keep the same airspeed that will cause a higher fuel consumption.

1.1.1 Characteristic ambient conditions at which icing occurs

As mentioned before super-cooled water droplets is water which can be in a liquid state even though the temperature is below 0°C due to the absence of freezing nuclei which can be small particles as dust, pollen or in this case, the aircraft's exposed surfaces. Super-cooled water droplets can exist at temperatures as low as -40°C and an interaction with a surface or substance is needed in order to initiate the freezing process. According to [2], "the shape of the accreted ice and its affect on the aircraft's performance depend on several parameters" being these parameters related with the weather conditions at which icing occurs and also related with the accreted body factors. The most influencing parameters and its effect on the ice accretion process are listed below

Cloud Types
The National Weather Service of the US government [3] divide clouds into three main categories: Strato-form, usually broad and fairly wide spread appearing like a blanket; Cumulo-form, which are generally detached and heaped up clouds which look fluffy and Cirro-form which are whitish and curly. The table below will show some of the characteristics of each type of cloud according to [4].

	Strato-form	Cumulo-form	Cirro-form
Liquid Water Content	Low liquid water content and small droplet sizes	High liquid water content	Composed entirely of ice crystals
Altitude	0-22,000 feet	4,000-30,000 feet	16,500-45,000 feet
Temperature Range	0 to -30°C	0 to -30°C	Below -30°C
Mean diameter water droplets	15-40 µm	15-50µm	
Types-precipitation	Stratus - Drizzle Stratocumulus - Light rain Nimbostratus - Rain and light rain Altostratus - Rain and snow	Altocumulus - Rain does not hit the ground Cumulus - Rain showers and snow/hail pellets Cumulonimbus - Heavy rain and thunderstorms	Cirrus Cirrocumulus Cirrostratus - (All produce only ice crystals)

Figure 1: Cloud Types and characteristics

As cirro-form clouds are located above 16,500 feet, their temperatures are the lowest of all, are composed primarily of ice crystals and therefore the conditions are given to not present icing risk.

[4] define the icing occurring in strato-form clouds as Continuous Maximum icing with the lowest liquid water content given from 0.04 to 0.15 g/m3 and the highest being from 0.2 to 0.8 g/m3. In this type of clouds rime ice is frequently formed and glaze ice can occur but less frequent. When ice forms at temperature ranges between 0 and -15°C the risk is considered the greater, if this happens below -15°C the risk is moderate and below -30°C there is a low risk. This is explained simply because at temperatures lower than -15°C supercooled water droplets are smaller and start to freeze instantaneously without the influence of freezing nuclei. Overall, Continuous Maximum icing imply low to moderate risk. That is the reason why sometimes to reduce aircraft icing risk it is advised to the pilots to climb into the much colder temperatures.

On the other hand, in the same article Intermittent Maximum icing is related with cumulo-form clouds which represent more risk for aircraft due to their rapid development and higher liquid content compared to Continuous maximum icing. The lowest liquid water content occurs from 0.4 to 0.1 g/m3 and the highest from 2.9 to 1.1 g/m3. When ice forms at temperature ranges between -3.3 and -20°C the risk is considered high, if icing happens below -20°C the risk is moderate and below -30°C the risk is low. Finally, for this clouds generally glaze and mixed ice occurs [5].

Droplet Diameter
Regarding droplet diameter, there can be existence of median size droplets or supercooled large droplets also known as SLD. [5] referring to FAR Part25 indicates that the median volumetric droplet diameter (MVD) range, for median size droplets, goes between 15 and 50 μm and explicitly indicates that "the change of drag coefficient and droplet trajectories are smaller than that of SLD (supercooled large droplets) conditions in which the MVD is over 40 μm" meaning that the MVD for median size droplets does not represent a big change in the icing accretion process or shape. Contrary to this, SLD which can reach sizes above 500 μm can represent very hazardous conditions for aircraft, meaning that icing protection systems may fail. The risk appear because of the capability of the droplets with larger MVD to cover and freeze at a greater extent of the surface that is not protected by the anti or de-icing systems on wings or tail of the aircraft and adhere to these. On the other hand smaller MVD means that droplets will follow the airstream and there is less probability for these to hit the surface or they can hit and freeze on the protected areas on the leading edges which is an advantage [1].

Liquid water content
Liquid water content (LWC) is one of the most important weather aspects when talking about ice accretion. LWC is defined as the density of liquid water in a cloud expressed in grams of water per cubic meter. Simply put, LWC indicates the amount of water that exist and is available for ice accretion. Generally speaking, the greater the water content the greater the rate of ice accretion although some aspects of the aircraft also determines this rate as the collection effieciency due to the shape of the aircraft and its speed.Cumulo-form clouds are unstable clouds and therefore a continuous movement of air occurs within these, implying higher energy presence which in turn results in a greater amount of supercooled droplets. Unlike cumulo-form, strati-form clouds are more stable meaning less energy and therefore lower amount of LWC [4].

Ambient Temperature
According to [5], ambient temperature has an important effect on the shape formation and shape changes of ice accretion. As said in previous paragraph at temperatures near -40°C mainly ice crystals are present so aircraft icing at this temperatures is not a problem but instead, higher temperatures near 0C represent a high risk. In the same study [5] states that at temperatures between -3 and -9°C the shape of the ice accreted areas start changing and at higher temperatures runback can occur. These factors lead to a more difficult prediction of an icing event. In this section the pressure altitude factor can be discussed as there is a direct relation between altitude and temperature. As altitude increases, temperature decreases reaching a minimum temperature according to [4] of -56.5°C at 36,089 feet who also mention that icing rarely occur above 22,000 feet.

Terrain Factors
Orographic factors or terrain factors have an influence on ice accretion due to their effect on cloud formations and air movement over for example mountainous terrains. Mountains and hills obstruct the normal movement of air and uplift it cooling its temperature and also provide additional support to the cloud, thus increasing the amount of supercooled water droplets. This lead to the formation clouds which can be cumulo or strato-form depending on the stability of the air masses within the cloud. This cloud formation can result in severe ice accretion.

Aircraft specific factors
Not only weather specific conditions are important when referring to ice accretion but also aspects concerning the aircraft itself as for example the shape of aircraft components, the speed of the aircraft. Considering the aircraft shape, the radii of aircraft parts may influence the collection efficiency, large curvature radii will lead to less collection of water while small curvatures will keep the airflow constant, therefore a higher water collection rate would be expected. Concerning speed, an increase of speed imply less time for the droplets to flow over the surfaces which can lead to an accumulation of supercooled droplets on the leading edges. Even though, [4] states that at velocities higher than 430 knots the aerodynamic heating overcomes the effect of mass flux when velocities are high and therefore structural icing becomes less risky. At speeds near and above 580 knots the author mentions that "structural icing ceases to be a problem" so it can be said that at velocities between 200 to 430 knots icing imply a risk. It should be stated that the higher the thickness-to-chord length ratio, the lower the total collection efficiency becomes. The chord length is the distance between the leading edge in front of the wing and the trailing edge at the backside of the wing.

1.1.2 Characteristics and icing types

Different types of ice accretion have different characteristics that tend to impact the performance of an aircraft in different ways. There are three main types of ice accretion, in this part the characteristics of each type will be explained.

Rime ice
The first one is what is determined as "Rime ice". For the formation of this type of ice the temperature must be below -10 degrees Celsius, and low concentration of water in the clouds must be present. The characteristics of this type of ice are: It presents a milky color which is due to the presence of high concentration of air bobbles trap inside the ice, very low temperatures tend to freeze the water droplets instantly preventing the air from escaping and forming ice with high air concentration. After a time the rime ice will present a spherical shape, according to [1] a "superhead appearance" in the front part of the airfoil. It has a high roughness surface (more than the roughness of the wing), this roughness is the responsible of reducing the aerodynamic efficiency of the airfoil. Also due to the air bobbles trapped it is normally weaker than other types of ice accretion.

Glaze ice
The second type of ice is called "Glaze ice". This ice accretion normally forms at temperatures ranging -10 and 0 degrees Celsius and in higher cloud water concentrations (Vukits,2002), because of more warm temperatures than rime ice, it have more time to slide through the surface of the wing before freezing. For this reason it can be found in the upper surface of the airfoil, [1] says that this will produce a "localized thickening" looking as a horn in each of the surfaces (upper and lower). It is stronger than rime ice due to the lower concentration of air bobbles that were drain during the freezing process, presenting a clear color.

Mixed ice
In reality, just one type of ice is not possible because of the various conditions at which the airplanes are exposed. Therefore most of the time both "Rime ice" and "Glaze ice" are present in the air-frame. This type of ice presents characteristics of both icing types, increasing the danger due to the combination of drawbacks of both. This type of ice usually presents the more transparent ice (glaze ice) in the narrow front of the airfoil, while the weaker and white ice (rime ice) is located at the upper surface of the airfoil.

1.2 Possible anti-icing systems

1.2.1 General definition of anti-icing systems

As mentioned in the last section, ice accretion threatens optimal aerodynamic performance in airplanes. Ice protection systems have been developed to reduce the dependence of aerial transport to weather conditions and minimize the risk of catastrophic events.

Ice accretion in airplanes is faced with two different approaches: anti-icing systems and de-icing systems. Anti-icing systems aim to prevent ice formation, delay it or ease later ice removal operations. On the other hand, de-icing systems remove ice once it has already formed [6]. It is worth mentioning that these two approaches are usually used simultaneously, and that one system can be either perform both functions.

Ice protection systems can be classified into two categories: active and passive.

1.2.2 Active Methods

"Active methods require an energy supply and use external systems such as thermal, chemical or pneumatic" (Dalili et al., 2009). These methods instead of just mitigate the adhesion of ice to the surface also remove the ice structure formed. To better understanding some methods will be explained.

Flexible pneumatic boots
This is a de-icing system used mainly on the leading edges of an airplane. Pneumatic boots are natural rubber bags that inflate and deflate successively with compressed air in order to break and release the ice by air flow and the force of gravity (Botura and Fisher, 2003). Botura and Fisher also show that it can work well at -10° C. Moreover, it is a relative economical system and requires a small amount of energy. On the

other hand, Seifert stated that reduces the aerodynamic of an airplane and it is needed a constant and severe maintenance.

Thermal anti-icing system
In this system the air is bled off from engine compressors into piccolo tubes routed through wings. It is required a heavy and overly complex structure for the air ducting. According to Battisti et al.(2006). It has a low thermal efficiency of approximately 30 percent. Another problem is that the system consumes high amount of power at high wind speed and low temperature. Besides those problems, this system is one of the most used because of factors like price, and effectiveness.

Another type of thermal anti-icing system uses electrically heated graphite foil laminate (heating mats) (Jasinski et al., 1998) applied to the leading edge. These systems have two zones of heat application. The first zone on the leading edge receives continuous heat; the second zone receives heat in cycles (similar to the pneumatic boots) to dislodge the ice allowing aerodynamic forces to remove it. Thermal anti-ice systems should be activated prior to entering icing conditions. One of the most important advantages of this system is the higher thermal efficiency which rounds the 100 percent due to the direct heating (Battisti et al., 2005).Maissan, (2002) noted as cited in [7] , as a disadvantage these systems present a higher imbalance in case of failure . Furthermore, in case of extreme weather conditions the blade heating power found insufficient (Peltola et al., 2003)"[7] .

Electromagnetic impulse de-icing
"Electromagnetic impulses create a magnetic field once current is liberated to the spiral coil" (Mayer, 2007). This causes an induced vibration pulses flex a metal abrasion shield and break the ice. As Mayer stated the benefits of using this system are: efficient, environmentally friendly and consumes low energy. Unfortunately the ice expulsion is a potential problem because the ice is broken but not removed from the surface.

Freezing point depressants or TKS de-icing system
The deicer chemical of ethylene glycol is used to prevent the ice accretion. The also called weeping-wing design uses small holes located in the leading edge of the wing or other critical surfaces of the aircraft. This antifreeze solution is pumped to the leading edge and weeps out through the holes. The solution chemically breaks down the bond between the ice and surface leaving the ice be removed by air flow and gravity. As a disadvantage is the weight that it is generated due to the tank where the solution is contained [8]. This system is used frequently for airplanes within the general aviation category due to the lack of power of a proper generator.

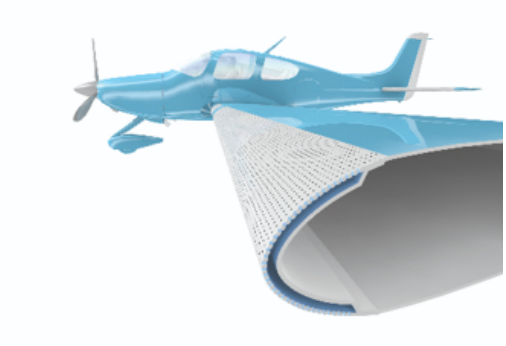

Figure 2: TKS System

Microwave
This system generates heat with microwaves to prevent ice formation on blade surface as [9] stated.Unfortunately, the energy loss can be considerably high if the microwave is transmitted through the air because a small fraction is capable to be intercepted by the surface. Therefore, "a dielectric surface waveguide is better in this respect, but it complicates the manufacturing procedures" (Salisbury, 1995)"[7]. In order to make the design functional it is needed to cover blade surface with a material that reflects microwaves [9]. Some tests were realized, for instance: Lm19.1 blade with a 6kW power and an emitted power less than 0.01 W/m2 (Mansson, 2004), but is not successfully implemented yet.

1.2.3 Passive methods

"Passive methods have the advantage of utilizing the physical properties of the blade surface to eliminate or prevent ice" [7]. From this, it can be concluded that no external energy is required since they rely on the surface's physical composition to fulfill anti-icing and de-icing functions. Some passive methods will be further explained down below.

Hydrophobic/superhydrophobic coatings
A surface can be considered hydrophobic if its water contact angle is >90°C and superhydrophobic if it is >150°C. This means a smaller contact area thus a lower ice adhesion strength. These surfaces also exhibit an ease for water droplets to roll off, specifically at 10°. Additionally this surfaces show a contact hysteresis angle smaller than 10° [6]. On the other side, it has been demonstrated that increasing liquid water content in the air or droplet diameters negatively impacts the effectiveness of this method [10]. [10] also stated that raising droplets impact velocity increases ice adhesion yet surface roughness is the strongest indicator for predicting adhesion. These results are explained considering the momentum of the droplets. [6] said that droplets with greater momentum can penetrate deeper into surface asperities, increasing effective contact area and adhesion strength.

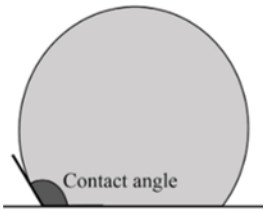

Figure 3: Contact Angle

High levels of humidity in the air at temperatures below freezing point, favors the creation of frost on the surface. Once this occurs, the surfaces becomes hydrophobic. Unfortunately, the performance of these surfaces is still limited by extreme weather conditions that usually wind tunnel tests are not able to replicate wholly accurate.

Icephobic coatings
It is important to note the difference between hydrophobic and icephobic surfaces. A hydrophobic surface is not by definition icephobic. This is because hydrophobic surfaces are not necessarily designed to impede or delay frost formation when dealing with supercooled droplets even though hydrophobic surfaces are generally good at maintaining low ice adhesion strength.

According to [11], a surface is considered to be icephobic if it fulfill three requirements: “prevent freezing of water condensing on the surface”, “prevent freezing of incoming water” and “ice formed should have low adhesion strength so it can be easily removed”. [6], an icephobic surface must have all the previous mentioned characteristics but also a specific adhesion strength of less than 100 kPa and for passive systems less than 20 kPa. This is due to the reliance of passive systems on aerodynamic forces to remove forming ice. These values are not universally agreed upon literature and when referring to a different source values change. For instance, ”Researchers call “icephobic” surfaces with the shear strength between 150 kPa and 500 kPa 2,15 and even as low as 15.6 kPa”. [12]

Three major forces must be considered when studying the bonding strength of droplets to the surface at molecular level: electrostatic forces, covalent bonds and Van Der Waals forces. [6]. First, electrostatic force has been shown to be directly proportional to ice adhesion hence materials with low dielectric constants are usually utilized in experiments. Second, chemical bonds and specifically hydrogen bonds show to have the strongest contribution to adhesion forces. Materials with low chemical compatibility with water must be chosen for icephobic porpoises.

[6] stated eight different categories for icephobic surfaces: Fluoropolymers, Biomimetic coatings, Nanotube coatings, Low cross link density, Liquid filled surfaces, Surface texturizing, Metallic, Siloxane Elastomers. Each of these types of surfaces has its strengths and weaknesses. For instance, metallic surfaces stand out by their erosion resistance in working environment while texturized surfaces are prone to it because of its topology delicacy. Other surfaces such as liquid filled surfaces use a low freezing point fluorinated liquid absorbed in the nanostructure to maintain a slippery condition. The idea behind these surfaces designed is to maintain surface’s intermolecular spaces filled with a fluid e.g. air, freezing point depressant or lubricant

such that droplets slip, or their freezing temperature drops below ambient conditions.

1.2.4 Key Performance Indicators

A performance indicator is a quantifiable measure of the level of success a system. For active systems are: energy efficiency, weight gain, functionality under risky conditions. As mentioned before, some systems like: the thermal (air bleed and electrical heat) and TKS sacrifices energy consumption and weight respectively in order to achieve its purpose. That is the reason of continuous experiments in order to optimize the anti-icing systems, for instance, the electromagnetic impulse or the microwave which both have higher amount of efficiencies but still need to be optimized to be entire functional.

Besides of the indicators mentioned before, another key factor is the price of the manufacturing process, is indeed for this indicator which provides another the factor of why pneumatic boots and TKS are commonly used on aircrafts.

In the case of ice protection passive systems, three determinant factors can be identified for passive systems: number of cycles the system will last, delay, humidity and temperature at which a frost layer will appear.

Commercial flight aircrafts' lifespan is usually between 25 and 30 years according to [13]. Cycles in airplanes are measured in pressurization cycles and this occurs every time the plane rises to its working altitude. Airplanes used for shorter trips experienced more frequently pressurization cycles. Thus, passive systems and specifically ice phobic surfaces or coatings most be designed to last as many cycles as possible to reduce costs. The reasonable number of cycles would be determined by the ease and cost of maintenance/replacement.

Humidity and temperature are dependent on the airplane working condition. An example given by [6] shows an icephobic surfaces can delay droplet freezing for 25 hours at -21° and 65% relative humidity. In order to find the most suitable system, all these three factors must be considered and compared to current Aerial regulations to find an optimal configuration.

1.3 Aviation certificate requirements

Each plane needs to fulfill certain requirements to be allowed to fly. In this part of the research the regulation of flight in conditions icing of a Boeing 737 have been studied to give an overview what is required of a plane flying in icing conditions. The following regulations are obtained from part 25-Airworthiness standards: Transport category airplanes of the FAA.[14].

1.3.1 certification types

There are two types of certificates related to flight in icing conditions. The first one is required when a plane should be able to fly in icing conditions. In general the plane needs to operate as normal when in icing conditions. For a plane that is not required to fly in icing conditions the regulations are different. The plane still need ice protection, so it can exit the icing conditions. But there are variations on this rule, for example it is possible for a plane to take of in icing conditions but not to fly in icing conditions for a long time.

1.3.2 Atmospheric conditions

There are three envelopes for types of atmospheric conditions: Continuous maximum icing (CM) and Intermittent maximum icing (IM). These two conditions respectively refer to the encounter with stratiform clouds and cumuliform clouds. There is also and envelope for maximum takeoff icing.

Continuous maximum icing (CM) and Intermittent maximum icing (IM)
The maximum continuous intensity of atmospheric icing conditions (continuous maximum icing) and the Intermittent maximum intensity of atmospheric icing conditions (intermittent maximum icing) are defined by the variables of the cloud liquid water content, the mean effective diameter of the cloud droplets, the ambient air temperature and the interrelationship of these three variables as shown in figure 40 (CM) and figure 43 (IM) of the appendix. The limiting icing envelope in terms of altitude and temperature is given in figure 41 (CM) and figure 44 (IM) of the appendix. The inter-relationship of cloud liquid water content with drop diameter and altitude is determined from figures 40 and 41 (CM) and figure 43 and 44 (IM). The cloud liquid water content for continuous maximum icing conditions of a horizontal extent is determined by

the value of liquid water content of figure 40, multiplied by the appropriate factor from figure 42 of this appendix. For Intermittent maximum icing, the cloud liquid water content is determined by the value of liquid water content figure 43, multiplied by the appropriate factor from figure 45 of the appendix.

Maximum takeoff icing
The maximum intensity of atmospheric icing conditions for takeoff (takeoff maximum icing) is defined by the cloud liquid water content of 0.35 g/m3. The mean effective diameter of the cloud droplets of 20 microns and the ambient air temperature at ground level of minus 9 degrees Celsius ($-9\ ^\circ$ C). The takeoff maximum icing conditions extend from ground level to a height of 1,500 feet above the level of the takeoff surface.

1.3.3 Ice protection system

A plane that flies in icing conditions needs an ice protection system to make sure that the plane can continue to fly as normal as possible for the duration of the flight, or to be able to exit the icing conditions. Examples for Ice protection systems are explained before.

Detection
The plane needs to be capable of detecting icing, this can be done by ice detection systems. Also a definition of visual cues which should alert the flight crew, examples of this are ice forming on the wingtips or on the windshield. When flying in the dark lights need to present to illuminate this spot.

Deicing
The Boeing 737 uses bleed air from the engine as ice protection system. Air is tapped form the engines and directed to parts of the plane that need to be de-iced. The ice protection system needs to be able to prevent ice forming on the plane and to remove ice that has formed on the plane. For a system that uses bleed air the holes where the air is blown out are prone to freeze if the system is not activated, the system should be able to clear the holes so the system can continue to operate.

1.3.4 Aircraft equipment

There are certain parts of the plane where icing could cause detrimental consequences, these part must be monitored closely to make sure that a flight in icing condition don't affect this part.

Anti-stall
When ice forms on an airplane this could result in a loss in lift, to increase the lift the angle of attack should be increased. So the sensor that measure the angle of attack should be heated to prevent malfunction due to icing. By increasing the angle of attack to much the plane will stall, the plane can't produce enough lift so it starts to descent. To prevent this a stall warnings system needs to be present. The stall warning in icing conditions needs to be provided by the same means as in non-icing conditions. When the stall warning is onset the pilot has a maximum of three second to start the recovery, the pilot should be able to recover the plane in this situation. Other equipment as the Speed indicator and Static pressure measurement equipment.

Engine
For regulations about the engines of the plane part 33-Airworthiness standards: Aircraft engines of the FAA [15]was consulted. The engine should operate as intended in icing conditions. There needs to be taken into account that the bleed air used for the de-icing of the aircraft results in a loss of thrust. The thrust generated when one engine is inoperative, in icing conditions, should be enough to let the plane climb. This is important after takeoff, so the plane can continue to fly in a safe manner.

1.3.5 Normative atmospheric conditions

The normative atmospheric conditions are used to calibrate aircraft equipment, the ideal standard atmosphere (ISA) is used to describe this.

Temperature
To determine the temperature at different altitudes the following can be used, in the troposphere the temperature decreases with a constant rate of 6.5 °C kilometer increase in altitude [16]. From this the following

formula can be derived, where T_0 is 15 °C, the temperature at sea level. The air is here considered as an ideal gas. In this formula means h(m) the height on a certain moment.

$$T = T_0 - 6.5\frac{h(m)}{1000} \tag{1}$$

Pressure
The determine the pressure at different altitudes it is assumed the temperature is standard and the air a perfect gas. The following formula is used to calculate the pressure at different altitudes.[16].

$$p = p_0(1 - 0.0065\frac{h}{T_0})^{5.2561} \tag{2}$$

Table of ISA
A table of ISA for pressures and temperature for different altitudes can be found in the appendix (Figure 46). [16]

1.4 Identification of the detailed problem

To be able to understand the importance of the various icing and geometrical parameters an identification of the detailed problem of ice accretion is performed. Icing on an aircraft is defined as flight in cloud at temperatures at or below freezing when supercooled water droplets impinge and freeze on the unprotected areas of the object on which they impact. The rate and amount of ice accretion on an unheated surface depends on the shape, including surface finish, the speed at which the body is travelling, the temperature, the liquid water concentration (LWC), the size of the droplets in the cloud and the size of the surface itself. Very small discontinuities on a smooth surface, such as dents, rivet heads and poorly aligned panel edges, can initiate ice growth on surfaces and in areas that would otherwise remain substantially ice free [1].

1.4.1 Fundamental factors for a realistic simulation

For this research the aim of in-flight icing is to precisely simulate the time-dependent ice accretion process. To be able to represent the ice accretion, three fundamental factors must be taken into account concurrently for realistic simulation. These are the representation of the aerodynamic flow-field (potential and viscous) characteristics on and around the body and growing ice accretion, the establishment of the water droplet trajectories with subsequent impingement characteristics and limits and the thermodynamics of the freezing/ice growth process [17].

FlowField
A simulation of the flowfield around and on the aerodynamic surface and potentially growing ice accretion is important for the analysis of how the flowfield will change, and thereby the water droplet trajectories will be affected. The flowfield determination results in two different circumstances. First the on-body (viscous) flow properties on the wing itself are essential for the heat transfer and distribution which have an significant influence on the ice accretion speed as well as the design requirements for anti-icing systems. The off-body flowfield is primarily important for the simulation of the water droplet trajectories.

Droplet trajectories
The droplet trajectories are necessary to be able to determine at what rate and which amount the water droplets are intercepted by the body. This is the product of the efficiency that the body collects the water (usually referred to as the water droplet collection or catch efficiency), the amount of water contained in the cloud (the cloud LWC) and the speed of the body through the cloud. The water droplet collection efficiency of the body is controlled mainly by the size and shape of the surface (especially the leading-edge radius) including the incidence. Droplet size is, however, the most important variable in the droplet trajectory simulation. These droplet sizes that are important to take into consideration for icing range from 10 to 400 micrometer [17]. The smaller the droplet size, the better it will tend to follow the streamline. However, as the droplet size increases, the inertia forces (proportional to the cube of the droplet diameter) become

dominant over the drag forces (proportional to the square of the droplet diameter) acting on the droplet. From this it follows that the droplets do not tend to follow the streamlines, and are therefore much more likely to impact the body. This will result in a greater collection efficiency [17]. Ambient pressure (altitude) and temperature have only a limited effect on the collection efficiency over the range of values appropriate to aircraft [1].

Thermodynamic/ freezing process
The last aspect to ice accretion is the rate at which the impinging water will freeze to form an ice buildup. This is primarily governed by the heat transfer from the surface of the body such as kinetic heating, convective cooling, evaporative cooling, latent heat of freezing and a number of smaller contributions from sensible heating and cooling mechanisms. For the impacting water droplets to freeze, their latent heat of fusion must be dissipated. The primary mechanisms of heat loss are normally convection and evaporation. The convective heat transfer is in practice largely controlled by the geometry and speed of the body in the airflow, the roughness of the iced surface and the ambient temperature difference that exists between the surface and the local air temperature. The operative cooling is a function of the vapour pressure of the water, which is itself a function of the temperature and the pressure at the surface. The pressure effect is through the enhanced concentration gradient that exists if the air is expanded and cooled, for example in the upper surface suction region of an aero foil or within an engine inlet [1]. In order to be able to make sure that the final design of an anti-icing system will perform well, the above mentioned subjects should carefully be looked into.

1.4.2 Problems with passive ice protection systems

According to [18] "erosion resistance is the biggest challenge for the coating industries." Here Fortin is reffering to the use of Passive Ice Protection systems (PIPS) on aircraft. Currently hydrophobic and super-hydrophobic coatings exist that work very well in protecting a substrate against the build up of ice. However, the use of these coatings on aircraft is still questionable: "There have been numerous attempts to develop durable superhydrophobic coatings to reduce water adhesion to surface or icephobic coatings to eliminate ice adhesion to surface, but all of them are not applicable on aircraft because none has been proven such that their resistance to erosion addresses the needs of the aircraft industry"[18].

1.4.3 Optimisation of anti-icing systems

It is not recommended to replace active ice protection systems (AIPS) with PIPS but instead to combine both systems. "If the ridge is eliminated by the superhydrophobic coating, thermal AIPS can operate in running wet mode rather than evaporation mode on the slat upper surface which would reduce the energy consumption of the thermal AIPS up to 20% for cold day and 80% for hot day. In addition, the energy gains in the lower surface which operates in running wet mode are lower, around 10%"[18]. Also as the AIPS uses less power, less fuel is needed to power it leading to a reduction in weight of the aircraft[18].

2 External flows and heat exchange

2.1 Path of a particle(droplet) in a flow

To determine whether a droplet will hit the airfoil, the velocity field around the airfoil was analyzed so the droplet trajectory could be computed.

2.1.1 Potential flow

To analyze the velocity field the airfoil, some assumptions have to be made. The airfoil is assumed to be a cylinder with a radius of R. The flow is assumed to be steady, incompressible, irrotational and inviscid. Futher there is assumed that the droplets don't affect the flow. By differentiating formula 3 ,with U the free stream velocity, formula 4 is obtained. With $\overrightarrow{u}$ the velocity field around the cylinder.

$$\phi(x,y) = Ux(1 + \frac{R^2}{x.^2 + y.^2}) \tag{3}$$

$$u = \frac{\delta\phi}{\delta x} \quad and \quad v = \frac{\delta\phi}{\delta y} \tag{4}$$

Using Matlab a figure was created to visualize the flow around a cylinder. See figure 4a.

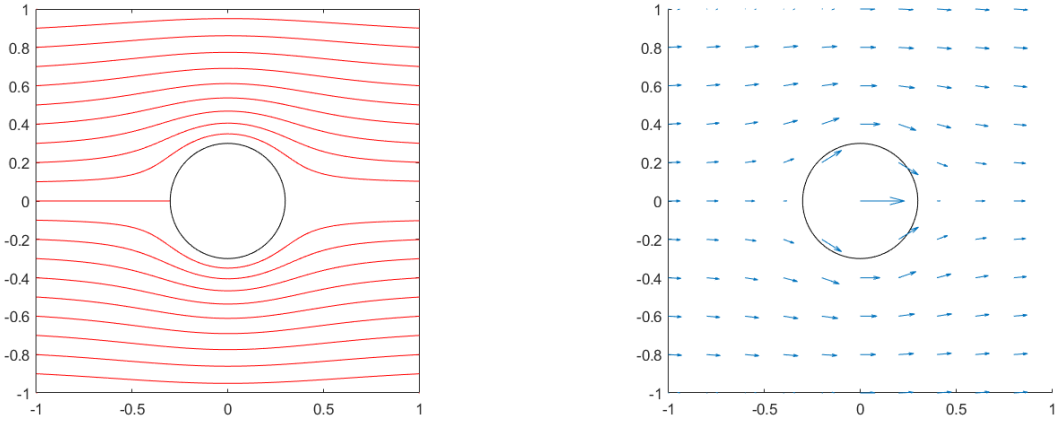

(a) streamlines around a cylinder

(b) velocity vectors around cylinder

Figure 4: flow around cylinder

In figure 4b there are also vectors displayed in the cylinder. These are not correct in real live the cylinder separates the flow inside from the flow outside, so the flow outside the cylinder doesn't affect the flow inside.

2.1.2 Droplet trajectory

To determine which droplets will hit the airfoil the trajectory of the droplets was computed. Some assumptions have been made to accomplish this, the droplets don't affect the velocity field, the droplets are perfect spheres whit a constant density, volume and the initial droplet velocity equals the free stream velocity. Newton's second law was used to model the path line of the droplets.The steady-drag force (equation 5) and the buoyancy force (equation 7) are usually used re used in Newton's second law [19].

$$F_{drag} = \frac{1}{2}\rho_a A_d C_D |\overrightarrow{u} - \overrightarrow{u_d}|(\overrightarrow{u} - \overrightarrow{u_d}) \tag{5}$$

$$F_g = \rho_d V_d \overrightarrow{g} \tag{6}$$

$$F_{bouy} = -\rho_a V_d \overrightarrow{g} \tag{7}$$

Using this equations in Newton's second law the path of the droplet can be computed.

$$\frac{d\overrightarrow{x_d}}{dt} = \overrightarrow{u_d} \tag{8}$$

$$m_d \frac{d\overrightarrow{u_d}}{dt} = \frac{1}{2}\rho_d A_d C_D |\overrightarrow{u} - \overrightarrow{u_d}|(\overrightarrow{u} - \overrightarrow{u_d}) + (\rho_d - \rho_a)V_d \overrightarrow{g} \tag{9}$$

This equation is rewritten using $\rho|\overrightarrow{u_a} - \overrightarrow{u_d}| = \frac{Re_d \mu_a}{d_{eq}}$ resulting in equation 10.

$$\frac{d\overrightarrow{u_d}}{dt} + \frac{C_D Re_d}{24}\frac{18\mu_a}{d_{eq}^2 \rho_d}(\overrightarrow{u_d} - \overrightarrow{u}) = (1 - \frac{\rho_a}{\rho_d})\overrightarrow{g} \tag{10}$$

Equation 10 was non-dimensionalized using $L_{ref} = c$, $U_{ref} = U_\infty$ and $t_{ref} = c/U_\infty$ resulting in equation 11.

$$\frac{d^2\overrightarrow{x_d}/L_{ref}}{d(t/t_{ref})^2} + 18\frac{C_D Re_d}{24}\frac{\rho_a}{\rho_d}\frac{\mu_a}{\rho_a \overrightarrow{U_\infty} c}\frac{1}{(d_{eq}/c)^2}(\frac{d\overrightarrow{x_d}/L_{ref}}{dt/t_{ref}} - \frac{\overrightarrow{u}}{\overrightarrow{U_\infty}}) = (1 - \frac{\rho_a}{\rho_d})\frac{\overrightarrow{g}c}{U_\infty^2} \tag{11}$$

This equation is rewritten using $\overrightarrow{\zeta_d} = \overrightarrow{x_d}/L_{ref}$ and $\tau = t/t_{ref}$

$$\frac{d^2\overrightarrow{\zeta_d}}{d\tau^2} + K(\frac{d\overrightarrow{\zeta_d}}{d\tau} - \frac{\overrightarrow{u}}{\overrightarrow{U_\infty}}) = (1 - \frac{\rho_a}{\rho_d})\frac{\overrightarrow{g}c}{U_\infty^2} \tag{12}$$

With

$$K = 18\frac{C_D Re_d}{24}\frac{\rho_a}{\rho_d}\frac{1}{Re_c}\frac{1}{(d_{eq}/c)^2} \tag{13}$$

K is the Langmuir parameter if this value is bigger the particle will tend to follow the streamlines. Here it can be seen that the droplet diameter changes the trajectory. For smaller diameters less hits will occur because the droplets follow the streamlines around the wing. This can be seen in figure 5a and figure 5b. The droplets are released at the same position, the larger droplets hit the airfoil where the smaller droplets are directed around the airfoil. This can be explained by using Newton's second law, a higher droplet diameter results in a higher mass. To accelerate that mass to change its direction will require more force compared to the lower diameter.

Equation 13 needs to be adjusted, in this form there is a very viscous flow which is not the case in this situation. With the following adjustment the equation is accurate for Reynolds number up to 1000.

$$\frac{C_D Re_d}{24} = 1.0 + 0.197 Re_d^{0.63} + 2.6 * 10^{-4} Re_d^{1.38} \tag{14}$$

Equation 12 was used to visualize the path lines of the droplet, see figure 5.

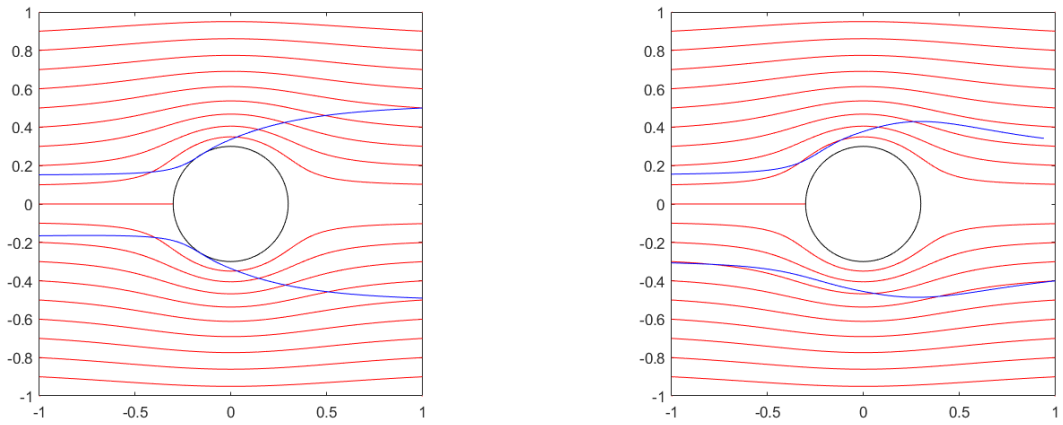

(a) Droplet with diameter of 40 μ m

(b) Droplet with diameter of 20 μ m

Figure 5: Path lines of a droplet

2.2 Mass and Energy balances

2.2.1 Control volume

The total amount of ice that will accrete on the wing at the aerofoil of the aircraft can be calculated using the appropriate mass and energy balances for small-scale control volumes located along the airfoil surface. By means of making use of the equations for continuity and energy conservation, for a steady flow and constant mass flow rates, of an infinitesimal control volume [19]. As can be seen from Fig. 6 where an overview is given of the control volume the following boundaries and coordinate system were set:

- Left boundary: $s = s_1$
- Right boundary: $s = s_2$
- Upper boundary: $y = h^+_{ice}(s)$
- Lower boundary: $y = h^-_{water}(s)$
- Vertical coordinate: y which denotes the height of the ice accretion.
- Horizontal coordinate: s which denotes the coordinate along the surface.

For clarification of the upper and lower boundary, the + and - sign indicate whether the boundary is located just above and just below the interface, respectively. The initial position for h^-_{ice} is located at the aerofoil itself, e.g. $h = 0$. Since the control volume is fixed, and the upper and lower boundary vary with time due to ice accretion on the aerofoil surface, the relative distance between h_{ice} and h_{water} remains equal. From this it follows that the control volume always will be located on the iced surface or on the aerofoil in the event happening that no ice accretion has taken place.

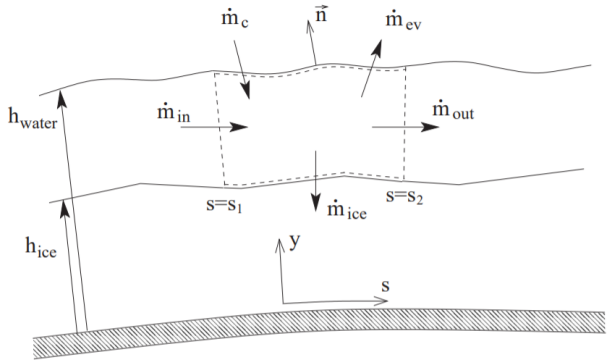

Figure 6: Control volume with mass flow rates

The previously made assumption that the control volume is infinitesimal results in that all physical variables can be assumed to be constant within the control volume. As can be seen from Fig. 6, the two terms $\dot{m}_{in}$ and $\dot{m}_{out}$ indicate that there is water transport going in and out of the control volume, respectively. Due to the fact that the water velocity is very small, the velocity can be neglected.

2.2.2 Mass conservation

The equation for the conservation of mass for water in an arbitrary control volume V with boundary S, moving with a velocity u_s and water speed u_w can be described as:

$$\frac{\partial u}{\partial t} \iiint_V \rho_w \, dV + \int_S \rho_w (\vec{u_w} - \vec{u_s}) \cdot \vec{n} \, dS = 0 \tag{15}$$

Where $\vec{n}$ is the outward pointing unit normal vector on the surface of the control volume. Making use of the assumption that quasi-steadiness applies to this situation, the term $\rho_w \vec{u_s} \cdot \int_S \vec{n} \, dS$ becomes zero, due to the fact of constant mass flow rates ($\vec{u}_s$ can be assumed constant in space).

$$\int_S \rho_w (\vec{u_w} \cdot \vec{n}) \, dS - \rho_w \vec{u_s} \cdot \int_S \vec{n} \, dS = 0 \tag{16}$$

Which can be shortened to:

$$\int_S \rho_w (\vec{u_w} \cdot \vec{n}) \, dS = 0 \tag{17}$$

The terms that contribute to the counter integral term are the mass flow of the run-back water in and out of the control volume, respectively: ($\dot{m}_{in}$) and ($\dot{m}_{out}$). Assuming that all the variables are constant, the following integrals can be derived for the mass flow:

$$\dot{m}_{in} = \int_{h_{ice}^+}^{h_{water}^-} \rho_w u_{in} \, dy \Big|_{s=s1} \tag{18}$$

$$\dot{m}_{out} = \int_{h_{ice}^+}^{h_{water}^-} \rho_w u_{out} \, dy \Big|_{s=s2} \tag{19}$$

An additional contour integral is required in order to resolve the mass flow of the contribution from the upper and lower boundaries of the control volume. Because the boundaries of the main control volume extend up to the ice and the air, there are two new infinitesimal control volumes introduced. The first infinitesimal control volume is partially in the ice and partially in the water. The second one is on the boundary between the air and the water. These control volumes couple the conditions on both sides of the main control volume to the boundaries of the main control volume itself. The assumption that no splashing takes place and that the phase-changes are instantaneous, is done in order to simplify the problem. The rate on which ice is formed is denoted by $\dot{m}_{ice}$ and the rate of evaporation is denoted by $\dot{m}_{ev}$. The mass flow of the water droplets that are caught by the surface is called $\dot{m}_c$ and is described by the following formula:

$$\dot{m_c} = LWC \cdot U_\infty \cdot \beta \cdot \Delta s \tag{20}$$

In this formula, LWC [kg/m^3] is the liquid water content of the air. Δs [m] is the length of the control volume along the surface. β is the dimensionless local catching efficiency.

The mass flow of the evaporating water is always dependent on the local temperature and the local pressure. In case there is completely no liquid water on the wing surface, it is still possible that evaporation takes place through sublimation of the ice. When this is the case, $\dot{m}_{ev}$ will be replaced by $\dot{m}_{sub}$, in order to specify the rate of mass transfer through sublimation.

As mentioned earlier, all masses contributing to the mass flows through the control volume are shown schematically in figure 6, with the unit $[kg/ms]$. The overall mass balance therefore logically results in:

$$\dot{m_{in}} + \dot{m_c} - \dot{m_{out}} - \dot{m_{ev}} - \dot{m_{ice}} = 0 \tag{21}$$

The process of ice accretion within the control volume can be described by a freezing fraction.

$$f = \frac{\dot{m_{ice}}}{\dot{m_c} + \dot{m_{in}}} \tag{22}$$

The freezing fraction (f) describes the fraction of the total mass of liquid entering the control volume that freezes within the control volume, and therefore can be described as above. The freezing fraction can take on different values as listed below:

- $f = 0.0$ indicates that no ice has formed.
- $0.0 \leq f \leq 1.0$ characterizes glaze ice or ice that has a combination of glaze and rime characteristics.
- $f = 1.0$ indicates cold (rime) icing conditions (zero runback water).

Important to mention is that the value of f can vary along the surface and can be calculated for every point of the surface with the use of the corresponding control volume and its mass and energy balance. The three possible phases of water on the wings can be seen in figures 7a, 7b and 7c.

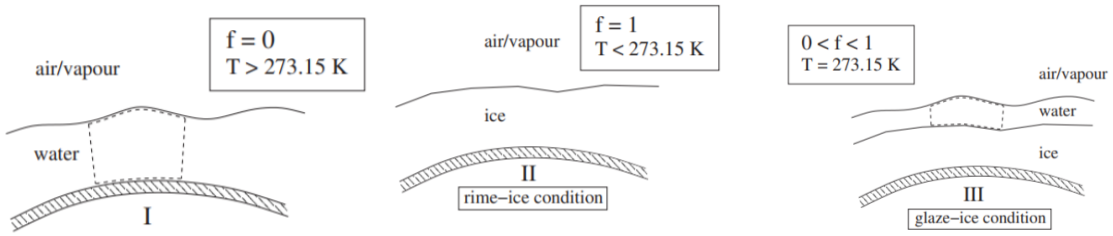

(a) Freezing factor with water (b) Freezing factor with ice (c) Freezing factor with water/ice

Figure 7: Caption

2.2.3 Energy conservation

The conservation of energy can be computed likewise the conservation of mass inside a control volume. See Fig. 8 for the most important heat fluxes.

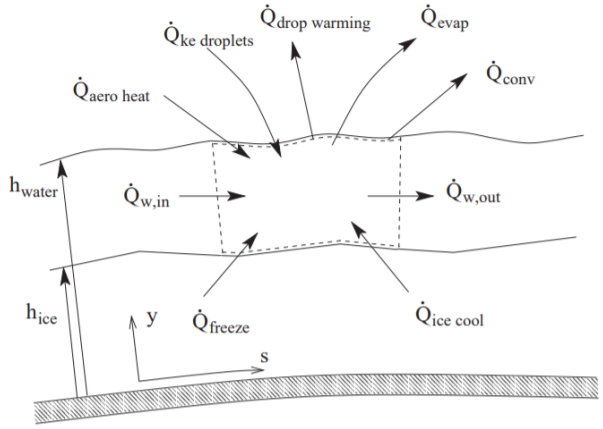

Figure 8: The heat fluxes of the control volume

When we neglect the work done by frictional forces within the water and the work done by external force fields and it is assumed that no volumetric heat sources are present, the energy equation is stated as follows:

$$\int_S \rho_w H_w (\vec{u_w} \cdot \vec{n}) dS = -\int_S \vec{q_w} \cdot \vec{n} dS \tag{23}$$

If in the enthalpy of the run-back water, which flows in and out of the control volume, the kinetic energy

is not taken into consideration. This leads to the next equations for enthalpy going in and going out of the control volume:

$$\dot{m}_{in} H_{w,in} = \int_{h_{ice}}^{h_{water}} \rho_w h_{w,in} u_{in} dy \Big|_{s=s1} \tag{24}$$

$$\dot{m}_{out} H_{w,out} = \int_{h_{ice}}^{h_{water}} \rho_w h_{w,out} u_{out} dy \Big|_{s=s2} \tag{25}$$

The expression for the heat flux by convection at the air/water interface is given by:

$$q_{conv} \Delta s = \int_{s_1}^{s_2} \vec{q}_{conv,w} \cdot \vec{n} ds \Big|_{h=h_{water}} \tag{26}$$

Radiative heat flux and the heat flux through the left-hand and right-hand boundary due to conduction are assumed to be negligible. Since ice is an insulator, the heat transfer between the water and the ice and the heat transfer between the ice and the airfoil skin will be very small and therefore neglected. When both ice and water are present on the airfoil, the temperature of the ice and the water will be T = 273,15K, therefore no convective heat flux between the water and the ice will be present. The right-hand side of Eq.23 is then given by:

$$-\int_S \vec{q}_w \cdot \vec{n} dS = -q_{conv} \Delta s \tag{27}$$

with:

$$q_{conv} = h_c (T_{sur} - (T_e + r \frac{U_\infty^2}{2 c_{pa}})) \tag{28}$$

in which h_c the heat transfer coefficient, r the recovery factor. The recovery factor r indicates the decrease of enthalpy due to viscosity losses. In an ideal situation, the value of r is equal to 1. However, due to viscosity losses, the value of r often lies between 0.8 and 0.9. T_{sur} the temperature of the water in the control volume, and T_e the temperature outside the control volume at the edge of the boundary layer, calculated from the pressure, calculated by the potential flow method using isentropic relations. The factor $\frac{U_\infty^2}{2c_{pa}}$ is the kinetic energy , where U_∞ is the velocity outside the control volume at the edge of the air boundary layer. Δs Is the length of the control volume along the surface.

Rewriting using substitution, as well as assuming the specific heat and that of ice to be constant. This gives using Eq.21:

$$\begin{aligned} \dot{m}_{ev} h_{WV/IV}^{T_{ref}=T} + q_{conv} \Delta s = {} & \dot{m}_c [c_{pw} (T_\infty - T) + \frac{U_\infty^2}{2}] \\ & + \dot{m}_{in} [c_{pw} (T_{in} - T)] \\ & + \dot{m}_{ice} h_{IW}^{T_{ref}=T} \\ & - \dot{m}_{ice} c_{pw} (T_f - T) \\ & + \dot{m}_{ice} c_{pi} (T_f - T) \end{aligned} \tag{29}$$

where T_{ref} is the reference temperature and $T = T_{sur} = T_{out}$. The subscripts all have their own meaning: w indicates the water phase, v indicates the vapor phase and i indicates the ice phase. $h_{WV}^{Tref=T}$ is the latent heat of vaporisation of water at temperature T, $h_{IV}^{Tref=T}$ is the latent heat of sublimation. All terms are in units of [W/m].

Eq. 29 can be expressed in two terms:

$$\dot{Q}_{source} = \dot{Q}_{sink} \tag{30}$$

in which $\dot{Q}_{source}$ represents the heat flux into the control volume, so fluxes which add heat to the volume, and $\dot{Q}_{sink}$ represents the heat flux out of the control volume, fluxes which extract heat from the volume.

When assuming the temperature of the air and the droplets is lower than the surface skin temperature, the sources of heat are:

$$\dot{Q}_{source} = \dot{Q}_{in} + \dot{Q}_{freeze} + \dot{Q}_{aeroheat} + \dot{Q}_{ke,droplets} + \dot{Q}_{icecool} + (\dot{Q}_{anti-ice}) \tag{31}$$

in which:

$$\begin{aligned} \dot{Q}_{in} &= \dot{m}_{in} c_{pw} (T_{in} - T) \\ \dot{Q}_{freeze} &= \dot{m}_{ice} h_{IW}^{T_{ref}=T} + \dot{m}_{ice} c_{pw} (T_f - T) \\ \dot{Q}_{aeroheat} &= h_c (T_e + \frac{U_\infty^2}{2c_{pa}} - T_\infty) \Delta s \\ \dot{Q}_{ke,droplets} &= \dot{m}_c \frac{U_\infty^2}{2} \\ \dot{Q}_{icecool} &= -\dot{m}_{ice} c_{pi} (T - T_f) \end{aligned} \tag{32}$$

Just as stated previously, $T = T_{sur} = T_{out}$. The heat flux due to conduction for the anti-icing system, $\dot{Q}_{anti-ice}$, will be elaborated in section 2.2.4.

The heat sinks are:

$$\dot{Q}_{sink} = \dot{Q}_{conv} + \dot{Q}_{dropwarming} + \dot{Q}_{evap} + \dot{Q}_{out} \tag{33}$$

in which:

$$\begin{aligned} \dot{Q}_{conv} &= h_c (T_{sur} - T_\infty) \Delta s \\ \dot{Q}_{dropwarming} &= -\dot{m}_c c_{pw} (T_\infty - T_{sur}) \\ \dot{Q}_{evap} &= \dot{m}_{ev} h_{WV}^{T_{ref}=T_{sur}} \\ \dot{Q}_{out} &= c_{pw} \dot{m}_{out} (T_{out} - T_{sur}) \end{aligned} \tag{34}$$

All terms substituted in Eq. 30 yields:

$$\dot{Q}_{in} + \dot{Q}_{freeze} + \dot{Q}_{kedroplets} + \dot{Q}_{icecool} + \dot{Q}_{aeroheat} (+\dot{Q}_{anti-ice}) = \dot{Q}_{conv} + \dot{Q}_{dropwarming} + \dot{Q}_{evap} + \dot{Q}_{out} \tag{35}$$

Important to mention is that some of the above stated heat sources have such a small contribution to the total heat flux into the control volume, that these can be neglected. The contribution of $\dot{Q}_{freeze}$ is remarkably small that it can be neglected. $\dot{Q}_{freeze} = \dot{m}_{ice} h_{IW}^{T_{ref}=T} + \dot{m}_{ice} c_{pw} (T_f - T)$

The term $\dot{m}_{ice} h_{IW}^{T_{ref}=T}$ can be assumed to be zero since the latent heat of sublimation, denoted by $h_{IW}^{T_{ref}=T}$, equals zero. As well as $\dot{Q}_{kedroplets}$ can be neglected, since the contribution to the total heat transfer is of such a small order. The term is described as $\dot{Q}_{ke,droplets} = \dot{m}_c \frac{U_\infty^2}{2}$, while $\frac{U_\infty^2}{2}$ the freestream velocity is defined as the speed in which the air infinitely far from the aircraft is moving when the object is kept as referential. The freestream velocity is, then, the velocity in which the aircraft is moving through the air and therefore not equal to zero. However due to the fact that $\dot{m}_c$ is of such a small order. The $\dot{m}_c$ shows a slight increase around the stagnation point, which is logical since the area around the stagnation point has the largest $\dot{m}_c$. Therefore Eq. 36 can be reduced to:

$$\dot{Q}_{in} + \dot{Q}_{icecool} + \dot{Q}_{aeroheat}(+\dot{Q}_{anti-ice}) = \dot{Q}_{conv} + \dot{Q}_{dropwarming} + \dot{Q}_{evap} + \dot{Q}_{out}$$

(36)

2.2.4 Anti-Icing

A well designed anti-icing system produces sufficient heat in order to prevent the impinging water from freezing onto the surface of the airplane. The heat can be produced by various heating applications (for several heating applications please refer to section 4). Anti-icing systems prevent ice accretion on the leading edge, and are thereby usually designed to evaporate a great amount of the impinging water. From this it follows that, within an anti-icing model, an additional term needs to be added to the energy balance (Eq. 29). Therefore the previously mentioned term $\dot{Q}_{anti-ice}$) comes into play in order for heat conduction through the aerofoil. See Fig. where $q_{anti-ice}\Delta s$ denotes the heat transfer at the bottom of the control volume.

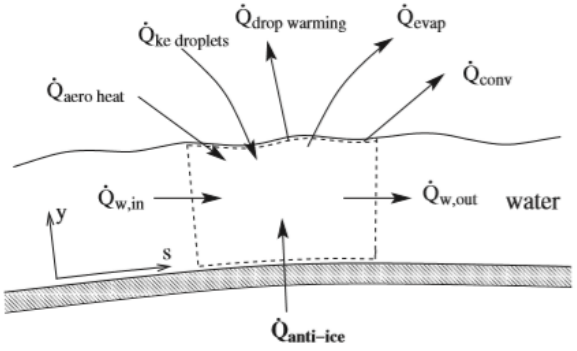

Figure 9: The heat fluxes in the ant-icing model.

From that it follows that the new heat balance, including $q_{anti-ice}\Delta s$, looks like:

$$\begin{aligned} \dot{m}_{ev} h_{WV/IV}^{T_{ref}=T} + q_{conv}\Delta s - q_{anti-ice}\Delta s = {} & \dot{m}_c[c_{pw}(T_\infty - T) + \frac{U_\infty^2}{2}] \\ & + \dot{m}_{in}[c_{pw}(T_{in} - T)] \\ & + \dot{m}_{ice} h_{IW}^{T_{ref}=T} \\ & - \dot{m}_{ice} c_{pw}(T_f - T) \\ & + \dot{m}_{ice} c_{pi}(T_f - T) \end{aligned} \tag{37}$$

Since the intend of this report is to design a anti-icing system, the assumption is made that $\dot{m}_{ice}$ is equal to zero, since no ice accretion should take place. When the situation does occur that ice is able to form, this will indicate that the delivered heat flux, $q_{anti-ice}\Delta s$, should be increased in order to make sure that the surface remains ice-free.

Using the above mentioned equations in combination with the mass and energy balances, the freezing factor and the type of water presence on the aeroplane wing can be predicted. Once the situation and consequences of water on the wing are known, and thus the accretion of ice, the hazards of ice on airplane wings can be minimized or as preferred prevented. Designing a device in the wings which accomplishes this, will require accurate and sufficient information about the formation of ice, which can be obtained through the mass and energy balances in the control volumes all over the airplane wings.

2.3 Worst case scenario

In order to develop an anti icing system, a worst case scenario has to be determined. This worst case scenario is the combination of atmospheric conditions that result in the highest amount of heat needed to keep the wing of the airplane free of ice. 2DFOIL-ICE is used to examine these atmospheric conditions and predict ice buildup and heat needed.

For the flight path of the plane, the holding phase is identified as being most high risk to flight build up. During take off and landing, the angle of of the wing is relatively high and this causes less ice build up. Whereas during cruising the Boeing 737 is about 41,000 Ft [20]. At this height, only cirro-form clouds are present (Figure. 1) which do not present an icing risk due as they consist of ice crystals. The holding phase of a flight path can take place between Minimum Holding Altitude(MHA) to over 14,000 Ft. At this altitude, Strato-form and Cumulo-form clouds are present (Figure 1) which cause more risk of icing due to the presence of sub-cooled droplets. The airplane usually flies at this altitude for around one minute when flying at or below 14,000 Ft or one and a half minute above 14,000 Ft respectively [21].

In 2DFOIL-ICE there are several parameters, that influence icing, which can be varied:

- Angle Of Attack [°]
- Free-Stream Velocity [m/s]
- Ambient Air Temperature [K]
- Ambient Pressure [Pa]
- Liquid Water Content (LWC) [kg/m^3]
- Droplet Diameter (MVD) [m]

From these values, angle of attack can be determined using the lift coefficient of the airplane, the ambient air temperature and ambient pressure are related to the altitude of the plane and the LWC and MVD are related to the ambient air temperature. As there is limited data on LWC and MVD based on temperatures, is was decided to use the temperatures from the LWC and MVD graph (figure 40 and figure 43) and use them as a basis to work with.

Figure 40 and figure 43 show data for the LWC and MVD. In order to calculate a worst case scenario, temperature values that occur in this figure should be used as a LWC and MVD value could be determined.

From the literature study it was found that for Strato-form clouds, the greatest risk of ice build up is at temperatures between 0 °C and -15 °C and for Cumulo-form clouds between -3.3 °C and -20 °C respectively. Therefore, the most risk of ice build up occurs at temperatures of 0 °C, -10 °C and -20 °C. The altitude at which these temperatures occur can be related to ambient pressure, the air density and the free stream velocity. This way three different scenarios can be determined and entered into 2DFOIL-ICE where a comparison can be made to find the worst case scenario.

The ambient air temperature is related to the altitude and the sea level standard temperature. This can be done by using equation 1 and solving for h. This way the altitudes of the temperatures can be determined. These altitudes are shown in table 3.

Using the values for temperature and altitude, the values for free stream velocity, pressure and the angle of attack can be determined. The formula for pressure is shown below in equation 38.

$$p = p_0 \cdot \left(1 - \frac{g \cdot h}{c_p \cdot T_0}\right)^{\frac{c_p \cdot M}{R_0}} \tag{38}$$

The free stream velocity of the airfoil can be set as the speed of the aircraft whilst flying at holding altitude. The maximum holding speeds at different altitudes above Mean Sea Level (MSL) and higher than Mean Holding Altitude (MHA) are shown in table 1 [22].

Altitude (MSL) [Ft]	Altitude (MSL) [m]	Airspeed [KIAS]	Airspeed [m/s]
MHA - 6000	MHA - 1828.8	200	102.89
6001 - 14000	1829.1 - 4267.2	230	118.32
14001 and above	4267.5 and above	265	136.33

Table 1: Maximum holding speeds at different altitudes

The angle of attack can be determined by calculating the lift coefficient needed to keep a Boeing 737 flying at the different holding altitudes. This can be done by using a force balance of a Boeing 737 where the lift force is equal to the gravitational force as shown in figure 10.

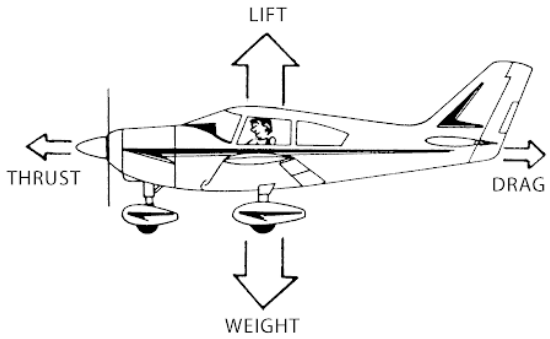

Figure 10: Forces on an airplane

From this figure, it can be derived that:

$$F_g = F_{lift} \tag{39}$$

$$m_{plane} \cdot g = \frac{1}{2} c_l \cdot \rho \cdot U_\infty^2 \cdot A_{wing} \tag{40}$$

This can be rewritten to calculate c_l

$$c_l = \frac{2 \cdot m_{plane} \cdot g}{\rho \cdot U_\infty^2 \cdot A_{wing}} \tag{41}$$

In order to find the value for c_l, ρ has to first be calculated:

$$\rho = \frac{p}{R_{specific} \cdot T} \tag{42}$$

Using the constants in table 7 all of the values from the formulas above can be calculated. For each scenario, the values for temperature, altitude, pressure, free stream velocity, density and the lift coefficient are shown in table 3.

The values for temperature, pressure, free stream velocity can be entered into 2DFOIL-ICE. By setting the value for "Number of ice accretion steps/layers" to 0, 2DFOIL-ICE will calculate the lift coefficient of the

airfoil from the given parameters and the angle of attack. Using this, the angle of attack van be varied and the lift coefficient that is calculated by 2DFOIL-ICE can be matched to the calculated a lift coefficient. This way the angle of attack can be found for each of the scenarios, the values for the angle of attack can be found in table 3.

Parameter	Description	Value
A_{wing}	Total wing area of a Boeing 737	127 m^2
c_p	Constant pressure specific heat	1 004.68506 J/(Kg·K)
g	Gravitational acceleration	9.81 m/s^2
M	Molar mass of dry air	0.02896968 kg/mol
m_{plane}	Fuselage mass of a Boeing 737	41 000 kg
p_0	Sea level standard atmospheric temperature	101 325 Pa
R_0	Universal gas constant	8.314462618 J/(mol·K)
$R_{specific}$	Specific gas constant for dry air	287.05 J/(mol·K)
T_0	Sea level standard temperature	288.16 K

Table 2: Constants for the formulas

Scenario	T [K]	h [m]	p [Pa]	U_∞ [m/s]	ρ [kg/m^3]	c_l	α [°]
1	253	5 409.2	49 877	136.33	0.68679	0.50	2.3
2	263	3 870.8	61 940	118.32	0.82046	0.55	2.9
3	293	2 332.3	75 955	118.32	0.96925	0.47	2.3

Table 3: Calculated values for each scenario

Now that these parameters are determined, the values for MVD and LWC can be determined. For each of the scenarios, the MVD is varied. Using data from figure 40 and 43 the LWC for any MVD can be determined using the temperature of the scenario. In order to find out which values for MVD and LWC would cause the most ice builup, the heat required to keep the wing at a fixed temperature above the melting point was determined. The MVD and LWC value that required the most heat would then be used for each worst case scenario. The values for MVD and LWC and the corresponding heat required are shown in figure 4.

Scenario	MVD [e^{-6} m]	LWC [g/m^3]	Heat required [kW/m^2]
1	20	1.700	164.04
2	20	2.200	151.28
3	15	0.800	1.68

Table 4: MVD, LWC and corresponding heat required to keep the wing at a certain temperature for each scenario

According to the data in figure 4, scenario 1 requires the most heat. As the wing temperature that requires this amount of heat and the area of the anti icing system are the same for each scenario, it can be assumed that the scenario which requires the most heat is the worst case scenario, which is then scenario 1. Table 5 gives an overview of the worst case scenario parameters that are used as an input for 2DFOIL-ICE.

Parameter	Description	Value
α	Angle of Attack	2.3 °
LWC	Liquid Water Content	1.700 e^{-}3 kg/m^3
MVD	Droplet Diameter	20 e^{-}6 m
p	Ambient Air Pressure	49 877 Pa
T	Ambient Air Temperature	253 K
U_∞	Free-Stream Velocity	136.33 m/s

Table 5: Worst case parameters in 2DFOIL-ICE

2.4 Ice accretion on an unprotected airfoil

To find out how different parameters affect the ice accretion, and analysis is done with 2DFOIL-ICE. In the previous section a worst case scenario was determined. The values of this worst case scenario are used to examine the ice accretion on the mid plane airfoil of Boeing 737. The parameters from table 5 are used unless they are varied for the sake of examining the ice accretion. For each parameters of the worst case scenario, a value higher and lower than the worst case scenario parameter is chosen and compared with the worst case value. The worst case parameter is represented by a red dashed line in each figure. The figures below are purely used to examine the difference in ice accretion when one single parameter is changed. MATLAB is used to process the data and plot the figures

2.4.1 Ice accretion for different temperatures

In figure 11 The ice accretion for different temperatures is shown. It can be seen that a higher ambient temperature allows the ice to spread out more over the airfoil. From this figure alone it is not fully clear whether a lower temperature causes more ice buildup as the lowest temperature causes a thicker ice layer over a small area. Where as for a higher temperature, the ice layer is thinner but spread out over a smaller area.

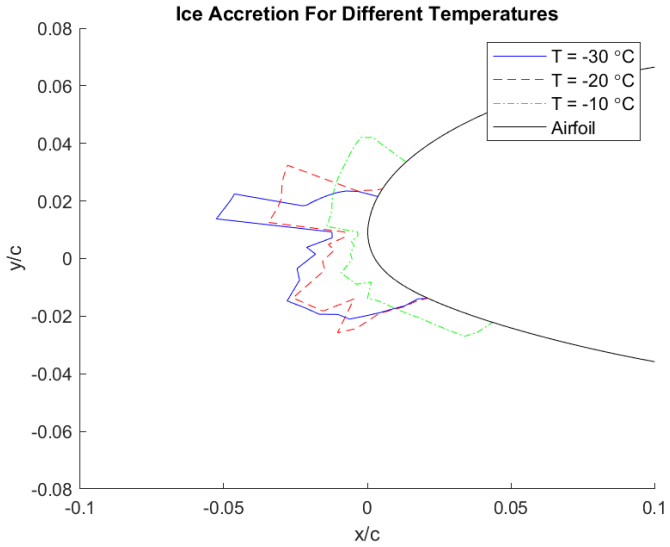

Figure 11: Ice Accretion for different Temperatures

2.4.2 Ice accretion for different LWCs

Figure 12 shows the ice accretion for different values of LWC. The figure shows that a greater value of LWC causes a thicker ice layer and more ice coverage over the airfoil. Therefore the LWC value greatly influences the ice accretion on an airfoil. The highest LWC value in this figure can not necessarily be used as a worst case scenario as this value may not appear like this in a real life situation.

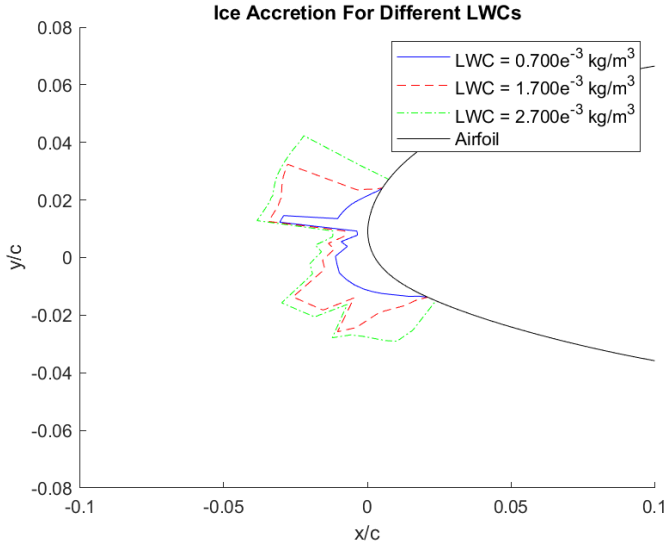

Figure 12: Ice Accretion for different LWCs

2.4.3 Ice accretion for different MVDs

Figure 13 shows the ice build up for different values of MVD. The figure shows that a higher MVD value has a big impact on the area covered by ice and also has a small relative impact to the ice thickness layer. In a real situation, the highest value of MVD does not necessarily cause the most ice buildup as a higher value of MVD relates to a lower value of LWC which could decrease ice accretion.

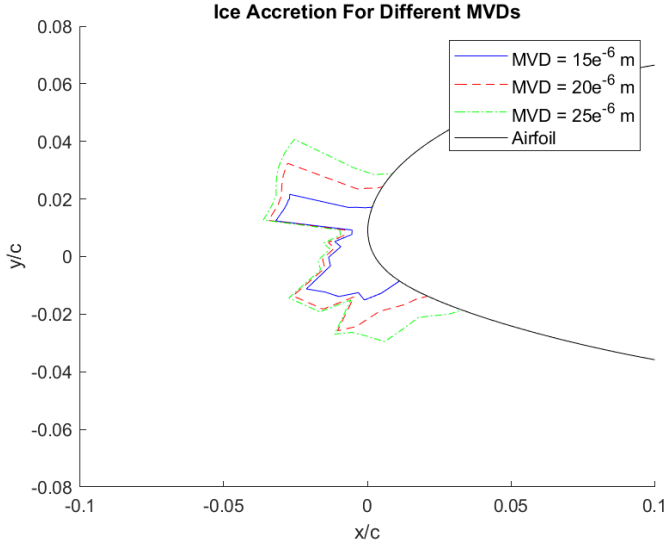

Figure 13: Ice Accretion for different MVDs

2.4.4 Ice accretion for different Free-stream velocities

Figure 14 shows the ice accretion for different free stream velocities which is the speed of the aircraft flying through the air. The figure shows that the biggest impact of a higher free stream velocity is the thickness of the ice layer further away from the stagnation point.

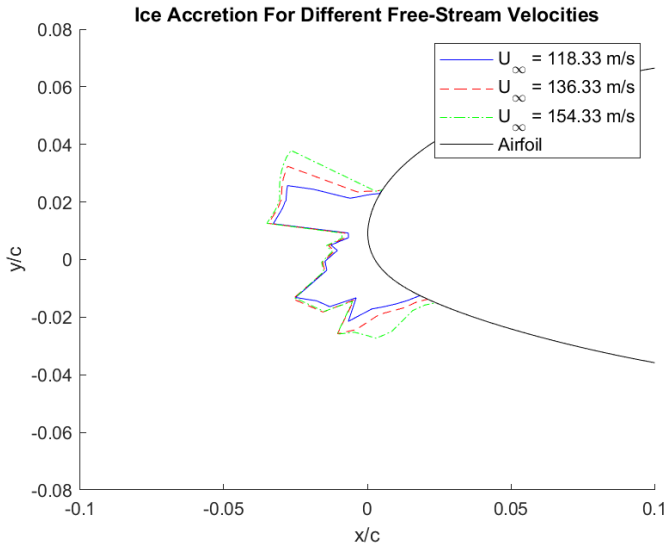

Figure 14: Ice Accretion for different Free-Stream Velocities

2.5 Heat transfer coefficient

To determine the heat flux, necessary to compare the results of the 2DFoil ICE with these calculated values, the heat transfer coefficient of the airfoil has to be determined. This heat transfer coefficient can be determined using different techniques. The surrounding conditions will be kept the same as used in 2DFOIL ICE. These conditions could be found in table 6.

Variable	Value
Nose radius	R1 = 0.0719 m
Wing radius	R2 = 0.2266 m
Cruise altitude	H = 5409.2 m
Cruise speed	U = 136.33 m/s
Angle of attack	$\alpha = 2.3$ °
Temperature	T = 253 K
Air density	$\rho = 0.68679$ kg/m^3
Dynamic air viscosity	$\mu = 1.614{\cdot}10^{-5}$ Pa· s
Coefficient thermal conductivity	k = 0.024 W/(m· K)
Heat capacity	$C_p = 1004.69$ J/(mol· K)

Table 6: Conditions

The heat transfer coefficient h_c can be determined with the Blasius solution of a flat plate. It is also possible to do this is by using the skin-friction coefficient in combination with the Reynolds analogy. For both ways, the airfoil has to be split in two flat plates and a cylinder up in front (see figure 15). The first cylinder approximation has a radius of the nose (R1). The second approximation is with the thickness of the airfoil (R2). The cylinder part will be determined using the local Nusselt number.

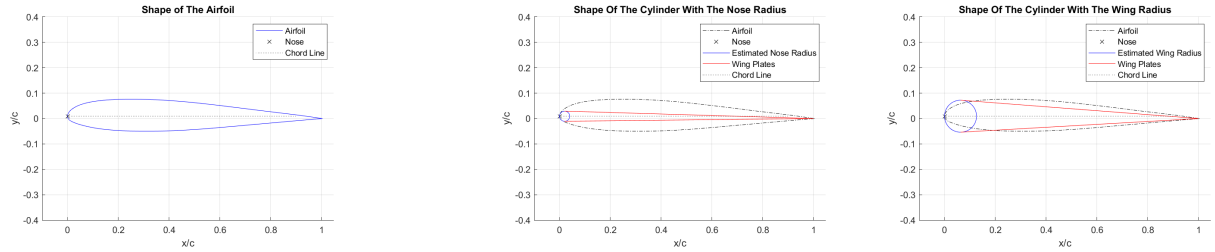

(a) Clear Airfoil (b) Estimated nose radius (c) Estimated wing radius

Figure 15: Airfoil of a cylinder with two flat plates

2.5.1 Cylinder

At first the cylinders heat transfer coefficient $h_{c,cyl}$ will be determined. The cylinder heat transfer coefficient can be determined using the Nusselt number. The Nusselt number is the ratio of total heat transfer to the conductive heat transfer. by rewriting this, equation 43 can be used to determine the heat transfer coefficient. [23]

$$h_{c,cyl} = \frac{Nu(s) \cdot k}{2R} \tag{43}$$

The Nusselt number has been determined for cylinders dependent on the Reynolds number in the stagnation point and the angular deviation from the stagnation point. To find the local Nusselt number,the Reynolds number of the stagnation point has to be determined. The Reynolds number is the ratio of the internal

inertial forces to the kinematic viscosity. The Reynold number calculation for both radii can be found in equation 44 en 45. [23]

$$R_{e_{R1}} = \frac{\rho U R1}{\mu} = 4.17 \cdot 10^5 \tag{44}$$

$$R_{e_{R2}} = \frac{\rho U R2}{\mu} = 1.31 \cdot 10^6 \tag{45}$$

The Nusselt number now can be found using some figures. For the first Reynold value ($R_e = 4.17 \cdot 10^5$) figure 16a can be used. One of the Reynold number in this figure is very close to the calculated value, so this corresponding line is used. For the second Reynold value ($R_e = 1.31 \cdot 10^6$) figure 16b can be used, because this Reynold value is very close to our value. The cylinder is joined by 2 flat plates at the top and bottom. Due to the angle of attack of 2.3 °, the plates start at 87.7 ° for the bottom plate and at 92.3 ° for the top plate. Therefore the data from the figures is needed between 87.7 ° and 92.3 °.[24]

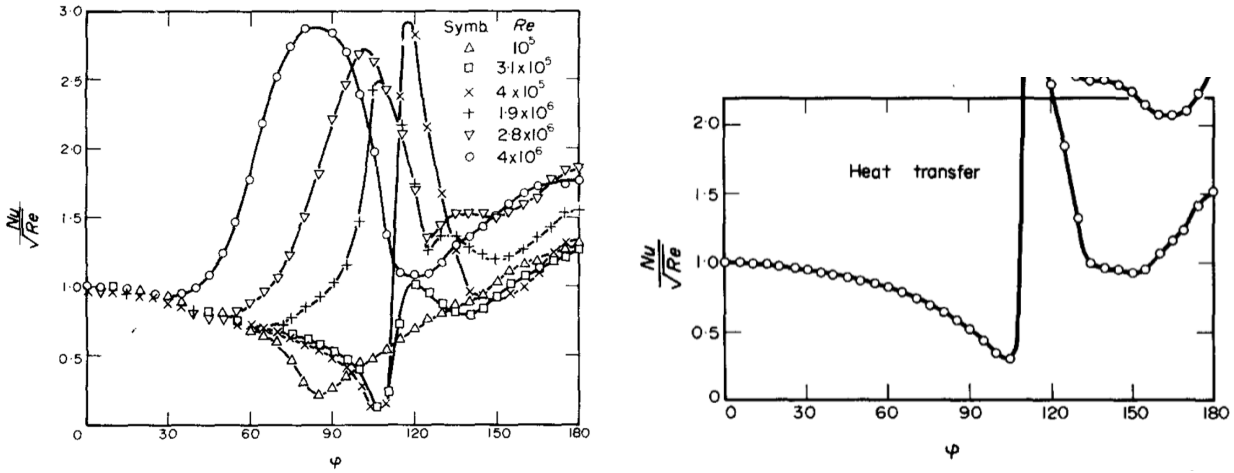

(a) Nusselt number for different Reynold number

(b) Nusselt number for $R_e = 1.27 \cdot 10^6$

Figure 16: Nusselt number graphs depending on the Reynolds number and the angular deviation

Assumed is that the Nusselt number for Re = $4 \cdot 10^5$ is a linear function from 87.7° till 92.3 °and that Re = $4.17 \cdot 10^5$ follows this line up to 92.3°, because these Reynolds values are very close to each other. Then the linear function found after several calculations is:

$$\frac{Nu}{\sqrt{R_{e_{R1}}}}(\theta) = -0.0130 \cdot \theta + 1.64 \tag{46}$$

For the other Reynolds value is the same assumed. Here is assumed that the Nusselt number for $R_e = 1.27 \cdot 10^6$ (figure 16b) is a linear function between 87.7° and 92.3°. This Reynolds number is so close to $R_e = 1.31 \cdot 10^6$ that the following linear function, corresponding to $R_e = 1.27 \cdot 10^6$, is used:

$$\frac{Nu}{\sqrt{R_{e_{R2}}}}(\theta) = -0.0163 \cdot \theta + 1.98 \tag{47}$$

An easier way to combine the flat plates and the cylinder is to use the Nusselt number as a function of the arc length instead of the angular coordinate. To rewrite the angular coordinate into the arc length equation is used. For the rewriting of the angular coordinate into the arc length, equation 48 is needed.

$$\theta = \frac{360s}{2\pi R} \tag{48}$$

When combining equation 48 with equation 46/47 and this is filled in into the final equation 43, the final equation for the heat coefficient as a function of the arc length over the cylinder can be found.

$$h_1 = \frac{(-0.013(\frac{360s}{2\pi R_1}) + 1.64) \cdot \sqrt{Re_{e_{R1}}} \cdot k}{2R_1} \approx -1116.5 \cdot s + 177.12 \tag{49}$$

$$h_2 = \frac{(-0.0163(\frac{360s}{2\pi R_2}) + 1.98) \cdot \sqrt{Re_{e_{R2}}} \cdot k}{2R_2} \approx -2.49.81 \cdot s + 120.16 \tag{50}$$

With these equations can be determined what the maximum heat coefficient is for the different radii, because this is when s = 0.

$$h_{1_{max}} = 177.12 W/m^2K \tag{51}$$

$$h_{2_{max}} = 120.16 W/m^2K \tag{52}$$

2.5.2 Blasius solution for the flat plates

To find the heat coefficient of a flat plate, the Blasius solution can be used. This is both calculated with a turbulent and a laminar boundary layer, but the calculated s value for the laminar boundary layer was so small, that this is an irrelevant result. This is the heat coefficient as a function of the position along a plate with a turbulent boundary layer [23]:

$$h_{Bl} = 0.0296 \frac{k}{s} Pr^{\frac{1}{3}} R_{e_s}^{\frac{4}{5}} \tag{53}$$

The Prandtl number (Pr) gives the ratio of kinematic viscosity to thermal diffusivity. [23]

$$Pr = \frac{\mu/\rho}{k/\rho C_p} = \frac{C_p \mu}{k} \tag{54}$$

R_{e_s} is here the Reynolds number at a certain point along the plate.

$$R_{e_s} = \frac{U \rho s}{\mu} \tag{55}$$

To find the match between the solution of the cylinder in combination with the blasius solution, the H_{bl} at the start of the flat plate on top of the cylinder must be the same as h_1 or h_2 at 92.3°. The same applies for the bottom plate, but her must H_{Bl} be the same as h_1 or h_2 at 87.7°. With these boundary conditions it is possible by using the Reynolds equation (equation 55) to find the values for s, where the curve changes from a straight line (plate) to your maximum value for the heat coefficient (h_{max}) and after back to a straight line. In this equation s gives the distance to the stagnation point. Figure 17 shows the Blasius solution combined with the solution for the cylinder for both different radii.

The top of figure 17a and figure 17b are the earlier calculated values for h_{max} on the cylinder and the straight horizontal lines are the heat capacity on the plates. These horizontal lines start at the calculated distance s from the stagnation point.

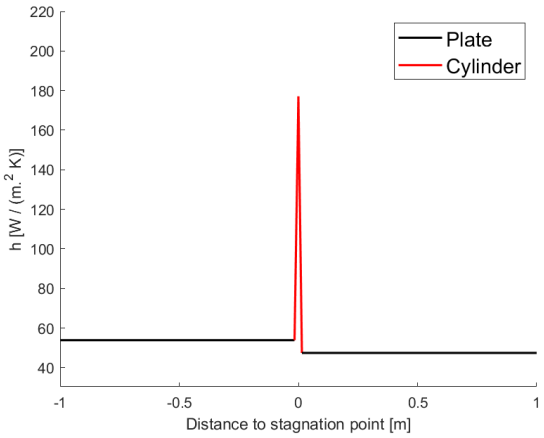

(a) Plot for heat capacity for nose radius

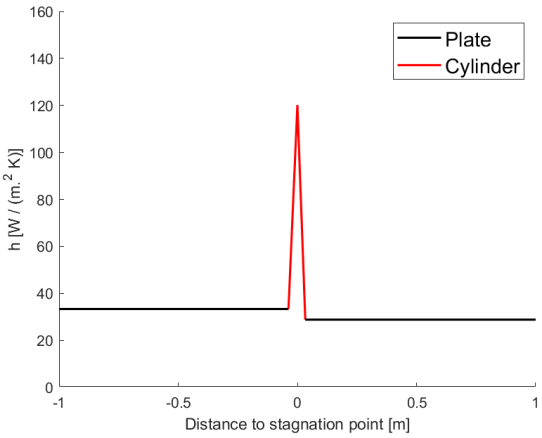

(b) Plot for heat capacity for wing radius

Figure 17: Figures for the heat capacity as a function of the distance to the stagnation point for the nose radius and the wing radius

2.5.3 Skin friction coefficient using Reynolds analogy

The heat transfer coefficient can also be determined using the Reynolds-Chilton-Colburn analogy, which is given by [23]:

$$\frac{C_{f,x}}{2} = Nu_x Re_x^{-1} P_r^{-\frac{1}{3}} \tag{56}$$

This equation can be rewritten as:

$$Nu_x = \frac{C_{f,x} Re_x Pr^{\frac{1}{3}}}{2} \tag{57}$$

In this equation is $C_{f,x}$ the local skin friction coefficient. This coefficient is different for a laminar flow and a turbulent flow. Equation 58 and 59 can be used to determine the local skin friction coefficient. [23]

$$Turbulent : C_{f,x} = 0.059 Re_x^{-\frac{1}{5}} \tag{58}$$

$$Laminar : C_{f,x} = 0.664 Re_x^{-\frac{1}{2}} \tag{59}$$

Now the already used formula to determine the heat coefficient can be used:

$$h = \frac{k Nu_x}{s} \tag{60}$$

To match the solutions for the heat transfer coefficient over the flat plate to the solutions of the cylinder, the heat transfer coefficient at the start of the plate should again be equal to the heat transfer coefficient at the end of the cylinder. This method is already explained earlier in the section. Figure 18 shows the heat coefficient for the nose radius and wing radius for a turbulent skin friction coefficient and figure 19 shows the heat coefficient for the nose and wing radius for a laminar skin friction coefficient.

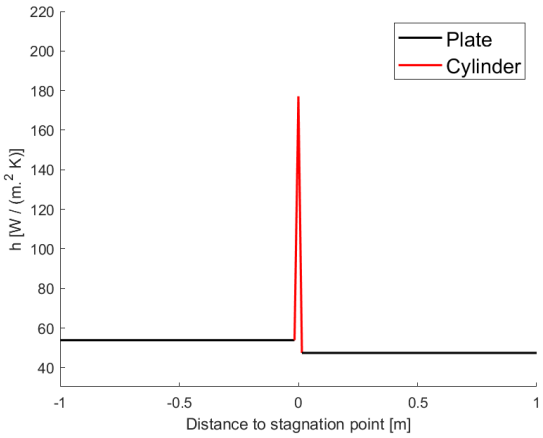

(a) Heat transfer coefficient using the turbulent skin friction for the nose radius

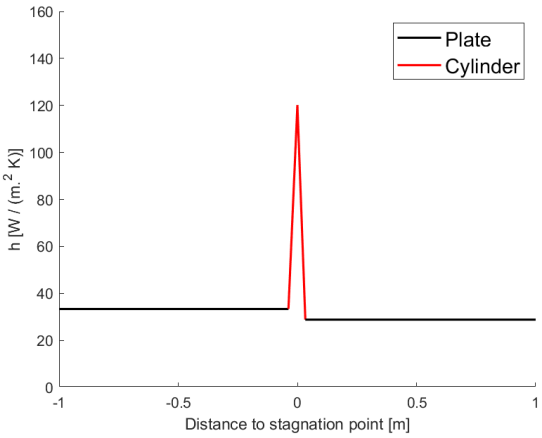

(b) Heat transfer coefficient using the turbulent skin friction for the wing radius

Figure 18: Heat transfer coefficient using the turbulent skin friction solutions

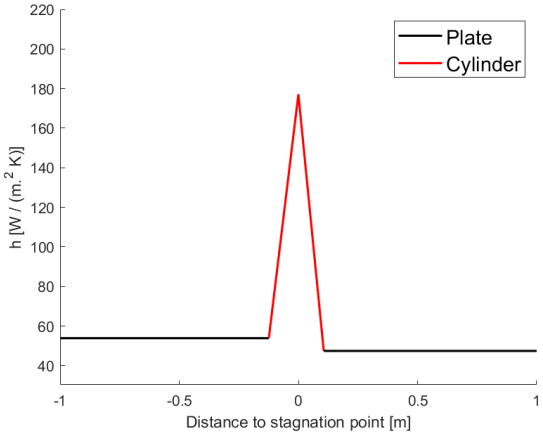

(a) Heat transfer coefficient using the laminar skin friction for the nose radius

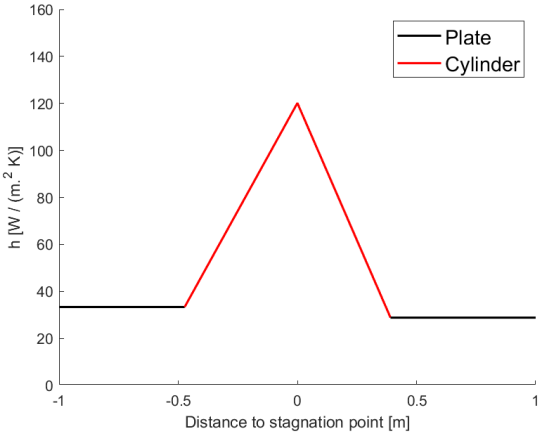

(b) Heat transfer coefficient using the laminar skin friction for the wing radius

Figure 19: Heat transfer coefficient using the laminar skin friction solutions

2.5.4 Comparing the 2DFOIL ICE solution with the calculated solutions

To figure out if the previous calculated solutions provide a good view of the heat transfer coefficient, a comparison is needed with the solutions by 2DFOIL ICE. Figure 20 shows the solution of 2DFOIL ICE.

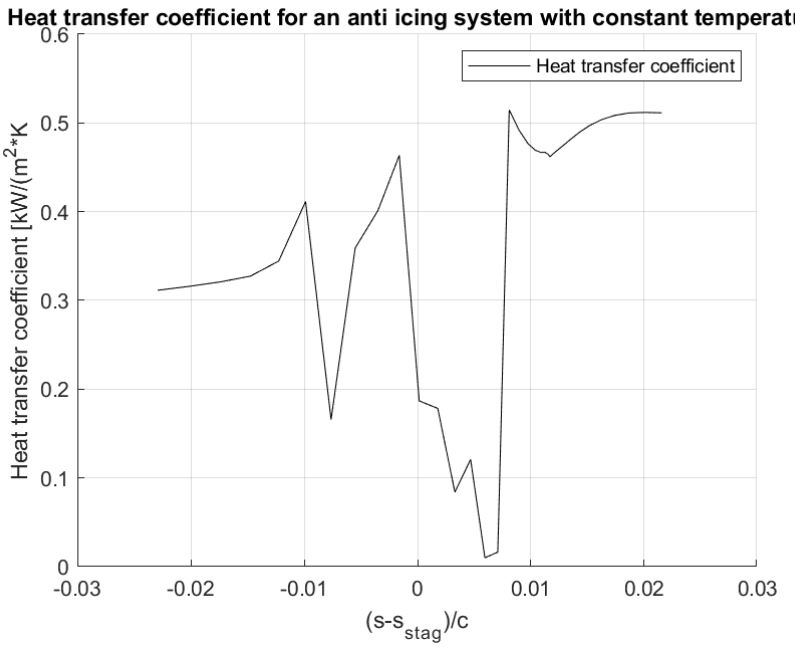

Figure 20: Heat transfer coefficient from 2DFOIL ICE

When look at the graphs it is noticeable, that the 2DFOIL ICE graph is shifting of near to the stagnation point. In none of the solutions of the calculated heat transfer coefficient these shifts are present. The shifts in the graph originate from the way 2DFOIL ICE calculates its heat transfer coefficient. Here the heat transfer coefficient is calculated by dividing the heat flux at a certain point by the temperature difference at that point. Next to the stagnation point, the anti-icing system stop heating the airfoil, that is creating these sudden increases. Another big different that comes up is the size of the heat transfer coefficient. In the 2DFOIL ICE graph the values range from 10 to 515 W/m^2K and the Blasius/skin friction graphs range from 28 to 177 W/m^2K. Also, the shifting from the cylinder to the Blasius flat plate solution and the friction solution is not as smooth as the 2DFOIL ICE graph. Both of these above mentioned observations can be explained by looking at the approximation of the airfoil for the calculations. This approximation is based of a cylinder and two flat plates. The way of determining the solutions and the used shape are very important for this approximation, because the heat transfer coefficient is very sensitive for this. Since the solution of the cylinder and the flat plates is not a uniform solution, but a combination of two different solutions, the sharp angle can be explained. Another important fact is that the airfoil has a smoother shape than the cylinder with two flat plates and this has a big impact on the heat transfer coefficient.

2.6 Heat Requirements

In order to determine the influence of different anti-icing systems, and to choose which one works best for our worst case scenario, the program 2DFOIL-ICE is used. 2DFOIL-ICE can simulate three different anti-icing systems:

- **Running wet system:** This system keeps the surface of the wing at a constant temperature.
- **Constant heat system:** This system provides a constant heat flux to the wing. Using this system the wall temperature can be varied as to be more efficient.
- **Fully evaporative system:** This system uses a combination of varying heat flux and wall temperature in order to fully evaporate all the ice on the airfoil.

All three systems are tested with the worst case scenario and they are compared by the total heat that is required to keep the protected area free of ice($\dot{Q}_{required}$).

In order to calculate the total amount of heat necessary to keep the protected area free of ice, the MATLAB function *trapz* is used. This function is used to integrate the values of anti-icing heat flux ($\dot{q}_{conduction}$) over the dimensionless distance from the stagnation point $\left(\frac{s-s_{stag}}{c}\right)$.

2.6.1 Running wet system

For this system the wall temperature over a protected area is set to be constant. The protected area is the area over which the anti ice system works, this is always located around the leading edge of the wing. The size of the protected area is kept as standard for a Boeing 737. The area itself is defined in 2DFOIL-ICE as the arc length coordinate normalized with the arc length form the nose to trailing edge. In simpler terms the percentage (as a decimal number) of the length between the nose trailing edge. They are defined for the top and bottom edge separately and both are set to 0.18. The wall temperature is set to 278K (5 °C). The heat fluxes calculated by 2DFOIL-ICE are shown in figure 21.

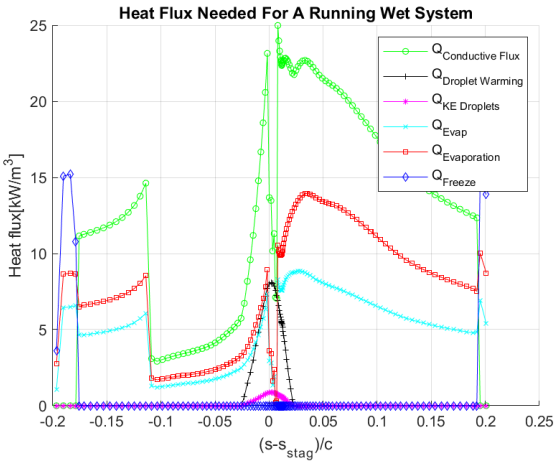

Figure 21: Heat flux for a running wet system

For this anti-icing system, the energy required to melt the ice is 4.84 kW/m^2. From figure 21 it is noticeable that $\dot{Q}_{Freeze}$ increases a lot right after the $\dot{Q}_{ConductiveFlux}$ drops to zero. This means that as soon as the melted ice droplets pass the boundary of the protected area, they freeze again. This "refreezing" of droplets could be affect the aerodynamic properties of the wing quite drastically and is therefore not safe. It could very well be that this anti-icing system works better at lower temperatures where the droplets may not refreeze whilst travelling over the airfoil.

2.6.2 Constant heat system

For this anti-icing system, the protected area is divided over 7 heating "pads". Each of these pads can output a different heat flux, this allows the system to output more heat to areas that accumulate more ice, which could make anti-icing more efficient. The position of these pads are defined as the distance from the nose over the airfoil and is measured in centimeters. To simulate this anti-icing system, a power density (kW/m^2) has to be specified for each pad. This power density is calculated by using the energy transfer equation 36 and solving it for $\dot{Q}_{anti-ice}$. This equation is then used with MATLAB to find the maximum power density needed per pad. These values can then be used an an input for 2DFOIL-ICE. The heat fluxes calculated by 2DFOIL-ICE are shown in figure 22.

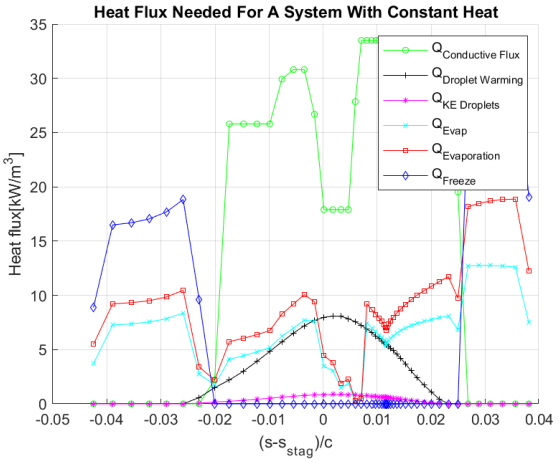

Figure 22: Heat flux for a constant heat system

For this anti icing system, the energy required to melt the ice is 1.23 kW/m^2. Similarly to the running wet anti-icing system, $\dot{Q}_{Freeze}$ increases a lot right after the $\dot{Q}_{ConductiveFlux}$ drops to zero, meaning that the water droplets freeze again right after the droplets travel outside the protected area. This means that this system would also not be safe in the worst case scenario.

2.6.3 Fully evaporative system

For this anti-icing system 2DFOIL-ICE calculates the heat flux necessary to fully evaporate all of the ice built up on the airfoil. It does this by deciding the most suitable surface temperatures and heat fluxes for each point on the airfoil. The heat fluxes calculated by 2DFOIL-ICE are shown in figure 23.

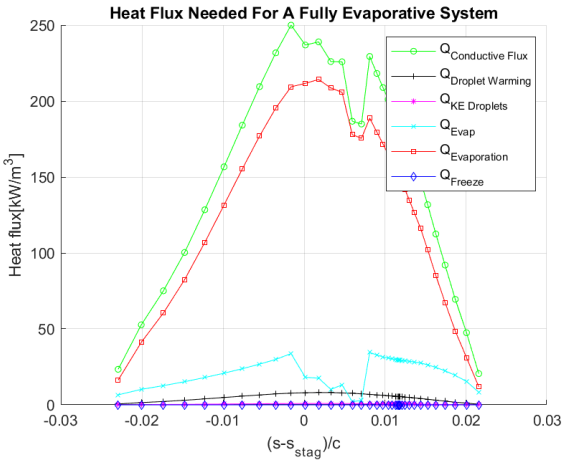

Figure 23: Heat fluxes for a fully evaporative system

For this anti-icing system, the energy required to melt the ice is 6.78 kW/m^2. This is much higher than the other two systems, however this is the only system much which melts all the ice. This means that this anti-icing system is the safest one out of the three and will therefore be used for the design of the anti-ice system.

2.6.4 Conclusion

Comparing the different anti-ice systems, the chosen system is fully evaporative. This is the only system out of three that manages to get rid of all of the ice. It may very well be that the other anti-ice systems are more suitable at higher ambient air temperatures where the droplets will not refreeze quickly after the ice has melted. The required heat to melt the ice ($\dot{Q}_{required}$) is 6.78 kW/m^2.

3 Internal flows and heat exchange

3.1 Electric heating mats

Heating mats exist in a variety of different models, and depends mainly in the type of airplane in which it is going to be used. In order to be more precise with the parameters needed to calculate the temperature differences through the wing, heating mats used in an Boeing 787 are going to be chosen as the model for this analysis. The temperature of these heating mats range between 7.2 °C and 21.1 °C with a power consumption of 150 to 200 kW [25], for this analysis the max temperature with the max power usage are going to be used. Also the area of the wing is 377 m^2, with this information the maximum heat flux is calculated with the next formula.

$$\dot{q}_{mats} = \frac{\dot{Q}_{mats}}{A} = \frac{200000}{377} = 530.5 W/m^2 \tag{61}$$

Other characteristics needed for this analysis are the material that is in between the heating mats and outside air, as can be seen in Fig. 24 the material used in the front of the airfoil is mainly Aluminum which has a conductive heat coefficient (k) of 205 W/mK. Heat transfer via radiation is negligible and therefore it is going to be ignored, and heat loss to the inside of the wing is negligible due to the insulator (Fig.25). The length of the wing span for this airplane is 60.1 m (from one point of the wing to the other) [26], because of the lack of information about the radius of the heating mats and thickness of the airfoil (Fig.25) they are going to be assumed as thickness 4 cm and radius 30 cm (R_2).

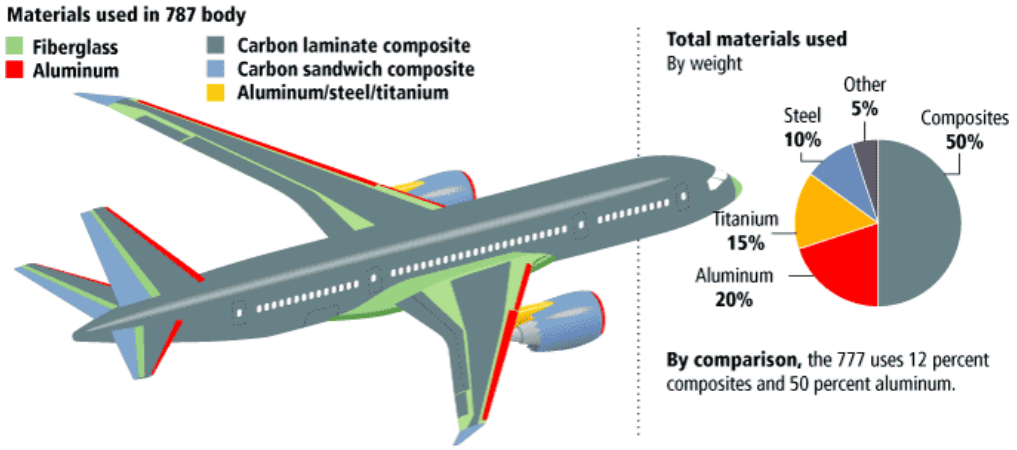

Figure 24: Representation of the materials used to construct the Boeing 787 Dreamliner.[26]

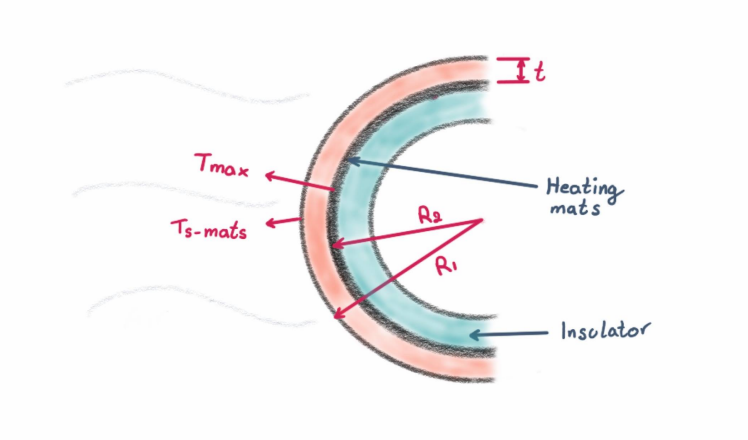

Figure 25: Representation of the front airfoil with Heating Mats

The process will consist of getting the temperature difference from the formula of heat transfer by conduction, then analyze if this change in temperature between the inner and the outer surfaces are high enough to be consider a major problem or if this is very small and can be ignored. The heating mats are going to be modeled as a half cylinder as in Fig. 25.

$$\dot{Q}_{mats} = \frac{2\pi Lk(T_{s-mats} - T_{max})}{\ln R_2/R_1} \tag{62}$$

Above is the formula of conduction through a cylinder, then it is rearranged to find $T_{s-mats} - T_{max}$, which is the temperature difference ($\triangle T$).

$$\triangle T = \frac{\dot{Q}_{mats} \ln R_2/R_1}{2\pi Lk} \tag{63}$$

Then the heat rate is replaced by heat flux.

$$\dot{Q}_{mats} = \dot{q}_{mats} A = \dot{q}_{mats} \pi DL \tag{64}$$

Gives,

$$\triangle T = \frac{\dot{q}_{mats} D \ln R_2/R_1}{2k} \tag{65}$$

The area is divided by 2 because just one half of a cylinder is going to be consider, so it give us.

$$\triangle T = \frac{\dot{q}_{mats} D \ln R_2/R_1}{k} \tag{66}$$

Values are: for R_1 is taken from R_2 + thickness ($R_1 = R_2 + t = 30cm + 4cm = 34cm$), the length of the wing is taken to be the half of the wing span for a Boeing 737-800 which is 35.8 m [27], giving a length of L = 17.9 m, diameter is $D = 2R_1 = 68$ cm, $k = 205W/mK$ and heat flux $\dot{q} = 530.5W/m^2$. After filling all the values, it is determined that $\triangle T = -0.22$ °C which is a very small change in temperature and therefore it will be neglected.

In order to determine if heating mats are a suitable solution as a deicing system, the heat flux found in 2DFOIL and the max heat flux provided by the heating mats is going to be compared. The first one is $\dot{q}_{2DFOIL} = 8.9130 kW/m^2$ and the second one is $\dot{q}_{mats} = 530.5 W/m^2$, these values show that heating mats does not provide enough heat to prevent ice formation on the airfoil.

Temperature difference along the wing (cordwise direction) will be neglected because heating mats are located just at the front of the airfoil.

3.2 Radiating surface from inside

Another type of heat transfer that will be analysed in order to proof whether or not it can be applicable and efficient enough to act as an anti-icing system is radiation. For the implementation of this analysis, some assumptions should be made.

Assumptions:

- The first is that convection and conduction are neglected, so only radiation is analyzed.
- The radiating object will be taken as a cylinder of radius r_{rad}, which is taken to be 0.1 meters which means it fits into the wing that has a radius of 0.3 meters as assumed previously on the part of external flows. This model is shown better in figure 26
- The material of the radiating object will be aluminium due to its good emissivity which is 0.77.
- As shown in figure 24, the material of the leading edge is Aluminium too.

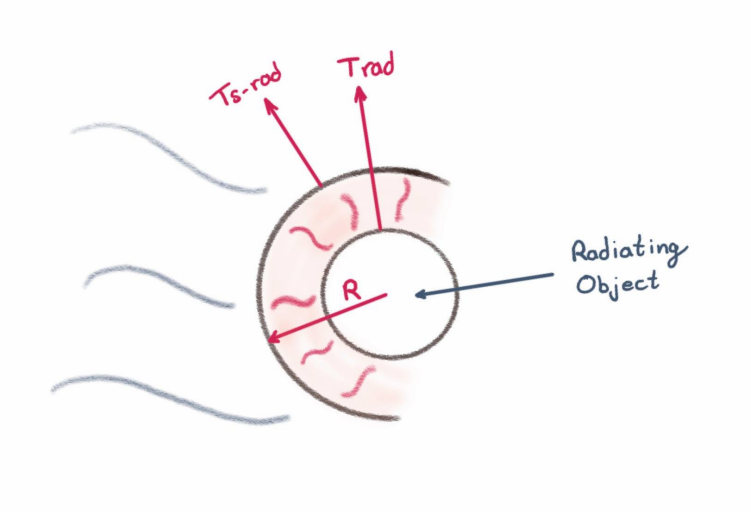

Figure 26: Representation of the radiating object inside the wing

For the process, radiation equations will be used in order to determine the temperature that the radiating object will need to have in order to transfer enough heat to the wing surface. Once this temperature is got, it can be compared to the maximum service temperature of the material, in this case aluminium, and see if the temperature is feasible or not. The following equation will be used, in which the radiation of the wing is subtracted by the one of the radiating object considering two infinitely long concentric cylinders:

$$\dot{Q}_{rad-wing} = \frac{A_{rad} * \sigma * (T_{rad}^4 - T_{wing}^4)}{1/\epsilon_{rad} + (1 - \epsilon_{wing})/\epsilon_{wing} * (r_{rad}/r_{wing})} \tag{67}$$

When analyzing radiation, the surface orientation of the surfaces relative to each other should be taken into account and expressed as a view factor inside the equation. The anti icing system, as previously mentioned, is modeled as half a cylinder, therefore the view factor that will be implemented is F_{1-2}=0.5. Then the equation remains as follows,

$$\dot{Q}_{rad-wing} = F_{1-2} * \frac{A_{rad} * \sigma * (T_{rad}^4 - T_{wing}^4)}{1/\epsilon_{rad} + (1 - \epsilon_{wing})/\epsilon_{wing} * (r_{rad}/r_{wing})} \tag{68}$$

After rearranging to get the temperature of the wing T_{wing} the final equation is given below,

$$T_{rad} = (\frac{\dot{Q}_{rad-wing} * (1/\epsilon_{rad} + (1-\epsilon_{wing})/\epsilon_{wing} * r_{rad}/r_{wing})}{F_{1-2} * A_{rad} * \sigma} + T_{wing}^4)^{1/4} \tag{69}$$

The table below shows the variables that will be used in the calculation,

Variable	Value
Temperature wing surface	$T_{wing} = 310k$
Radius radiating object	$r_{rad} = 0.1m$
Area radiating object	$A_{rad} = 2\pi r_{rad} l$
Radius leading edge of the wing	$r_{wing} = 0.3m$
Stefan-Boltzmann constant	$\sigma = 5.67 * 10^{-8} W/m^2 K^4$
Emissivity	$\epsilon = 0.77$
View Factor	$F_{1-2} = 0.5$
Needed heat	$Q_{rad-wing} = 65.2kW/m$

Finally, the result is $T_{rad} = 1505k$ which compared to the maximum service temperature of aluminium which is $623k$ end up being very high and even considering the melting temperature of aluminium which is around $873k$ it can be concluded that radiation is not a solution for the problem of this project. Taking another approach, the equation could be used to get the radius that the radiating object would need in order to transfer enough heat to the wing, after a rearrangement of the equation the result shows that a radius $r_{rad} = 17.31m$ would be needed and it is impossible to fit this inside the wing of the Boeing 737. Radiation is discarded as a possible method for an anti-icing system.

3.3 Natural convection

This section will analyze now, if heat transfer via natural convection can be used and implemented as an anti-incing system for this project. It should be mentioned that convection is usually accompanied by radiation but in this case both analysis are done separated. Thus, radiation is neglected now and the process start with setting up the model to be used.

If a fluid is heated and located inside the wing of the Boeing 737, as the wing is exposed to very low temperatures, natural convection will occur. Therefore the warm fluid will heat the wing surface trough natural convection currents. For this purpose, the model is taken to be as in the Radiation part, two concentric cylinders located as shown in figure 26, where the outer cylinder represents the wing surface and the inner cylinder represents a hot tube which will be transferring heat only via convection. Thickness of the wing is not taken into account and the fluid considered is air.

According [23] the natural convection heat transfer equation between two concentric cylinders is written as follows,

$$\dot{Q} = \frac{2 * pi * k_{eff}}{\ln(\frac{D_2}{D_1})} * (T_1 - T_2) \tag{70}$$

Where, k_{eff} is the effective thermal conductivity, D_1 and D_2 are the inner and outer diameters of the tube respectively, as well as T_1 and T_2 but with temperatures. It should be noticed that both cylinders are taken to be infinitely long and diameters can be simplified by the terms r_1 and r_2 which means only radius could be used in the equation.In order to get K_{eff}, the following relation is used,

$$\frac{k_{eff}}{k} = 0.386 * (\frac{Pr}{0.861 + Pr})^{1/4} * (F_{cyl} * Ra_L)^{1/4} \tag{71}$$

Where, Pr is the Prandtl number, F_{cyl} is the geometric factor for concentric cylinders and Ra_L is the Rayleigh number. The geometric factor can be obtained by the equation,

$$F_{cyl} = \frac{\ln(\frac{D_2}{D_1})^4}{{L_c}^3 * (D_1^{-3/5} + D_2^{-3/5})^5} \tag{72}$$

Where, $L_c = (D_2 - D_1)/2$ is the characteristic length. Most of the values were already given on the previous section of Radiation, except the Rayleigh and Prandtl numbers, which are dimensionless numbers that represent the relationship between buoyancy and viscosity the relationship between momentum diffusivity and thermal diffusivity respectively [23]. The equations to get these numbers are,

$$Ra_L = \frac{g * \beta * (T_1 - T_2) * L_c^3}{v * \alpha} \tag{73}$$

$$Pr = \frac{v}{\alpha} \tag{74}$$

All of the equations have been listed and now the variables will be shown in the table below, after this the heat transfer via natural convection will be calculated.

Variable	Value(Air)
Temperature wing surface	$T_2 = 310k$
Temperature hot object	$T_1 = 527k$
Radius hot object	$r_1 = 0.1m$
Radius leading edge of the wing	$r_2 = 0.3m$
Coefficient of thermal expansion	$\beta = 2.38 * 10^{-3} 1/k$
Thermal diffusivity	$\alpha = 3.898 * 10^{-}5m^2/s$
Gravity	$g = 9.8m/s^2$
Kinematic viscosity	$v = 2.745 * 10^{-5}m^2/s$
Prandtl number	$Pr = 0.7041$

Finally, it should be mentioned that equation only works if is described by the following equation if the Rayleigh number times the geometric factor is between 100 and 10^7 which is the case. The process continues with the equation and k is obtained from the table of air properties at the average temperature of $(T_1+T_2/2 = 418$, so $k = 0.03374W/mK$ deriving in $k_{eff} = 0.96$ The final result is $\dot{Q} = 111W/m$ which compared to the needed $\dot{Q} = 65.2kW/m$ end up being not sufficient in order to de-ice the surface and it can be concluded that natural convection is not a solution for the problem of this project. Natural convection is also discarded as a possible method for an anti-icing system.

3.4 Forced convection

Forced convection along the spanwise direction of the wing will be analyzed as method to keep the leading edge warm thus impeding ice accretion. The system consists in a pipe placed in spanwise direction and concentric to the of curvature of the leading edge. This will carry bleed air extracted from the compressor of the engine.In this section the mass flow required to provide the specified heat flux in 2D foil ice will be calculated. Then, it will be determined if the engine would be able to supply it.

Assumptions:

- Steady operations conditions exist.
- As considered in section 5.1 for electric heating mats, the leading-edge diameter of curvature. The analysed pipe is $0.6m$ will have the same radius.
- The thickness and thermal resistance of the pipe is negligible and its inner surface is smooth.
- Air is an ideal gas with constant properties.
- According to [28], bleed air temperature is often between 200 and 250 °C. For this analysis, the temperature at which it enters the wing (T_i) is 200 °C.
- Heat is only transferred through one half of the pipe, the other half is assumed to be insulated. Heat flux across the pipe is one-dimensional and uniform along its length.
- According to [29], the Boeing 737 has a wingspan of 35.8 m. This is a good example of a typical commercial aircraft. The wingspan is measured from the tip of one wing to the other including the cabin. It must be considered that the wings are not perpendicular to the cabin. Assuming values for angles and cabin width, the wing length is determined to be 17.9 m. The air will flow entirely along this distance.

Unfortunately, the exit temperature of the fluid can not be assumed.However, it is possible to obtained a relation of it as function of mass flow. Using the following equations and assuming that all the energy lost by the fluid is transferred to the outer surface. Also assuming that the arithmetic mean is accurate enough for this analysis.It is acceptable for temperature differences not larger than 40%. The validity of this assumption will be checked later.

$$\dot{Q} = \dot{m}C_p(T_i - Te) \tag{75}$$

$$T_{avg} = \frac{1}{2} * (T_i - T_e) \tag{76}$$

The relation of exit temperature and mass flow is obtained:

$$T_e = T_i - \frac{-\dot{q}A_s}{\dot{m}C_p} \tag{77}$$

This relation can then be replace in the formula for heat flux by convection:

$$\dot{q} = h\triangle T = h(T_{mean} - T_s) \tag{78}$$

Replacing and rewriting for h. The relation for heat transfer coefficient and mass flow is determined:

$$h = \frac{2\dot{q}}{T_i - \frac{-\dot{q}A}{\dot{m}C_p} - 2T_s} \tag{79}$$

Heat transfer coefficient can also be written using Dittus-Bolter equation for pipes. The flow is considered fully developed and turbulent. This assumption will be later checked.

$$Nu = \frac{hD}{k} = 0.023Re^{0.8}Pr^{1/3} \tag{80}$$

where Reynolds Numbers is:

$$Re = \frac{VD}{v} = \frac{\dot{m}}{v\rho} \tag{81}$$

Then:

$$h = \frac{0.023(\frac{\dot{m}}{v\rho})^{0.8}Pr^{1/3}k}{D} \tag{82}$$

The final step is to equate both equations of heat conduction coefficient and solve for the mass flow. At this point the properties of the air are required. Unfortunately, this can not bet determined with total accuracy since the outlet temperature has not been yet obtained. Therefore, a mean temperature for the air flowing along the tube is estimated to be 180 °C. According to [23]:

Properties of air at 180 °C and 1 atm	Value
Specific Heat (C_p)	1019 J/KgK
Density(ρ)	0.7788 kg/m^3
Thermal conductivity(k)	0.03646 W/mK
kinematic viscosity(v)	3.212e−5 m^2/s
Prandtl Number(Pr)	0.6992

Finally, mass flow is determined to be 28.5 Kg/s. The values for the exit temperature and Reynolds number are checked. (Te=159.88 ,Re = 1.14e6. According to [30], the mass flow of a turbo fan engine is 115 kg/s. The mass flow required for this system would be 24.77% of the total engine input. Anti-icing by forced convection is not a viable choice.

3.5 Impinging jets

Jet impingement is a heat transfer system which has relative high performance. This system is located inside of a wing of an airplane and a tube that cross all the way along the wing called piccolo tube. Hot bleed air goes through this tube which has small holes pointing the leading edge of the wing. Through these holes jet hot bleed air to keep the temperature on the wing.

Variable	Value
Bleed air temperature (T_i)	424 K
Surface temperature (T_s)	(310)K
Thermal conductivity coefficient(k)	0.03746 W/mK
Specific heat of air (Cp)	1023 $J/(kg.K)$
Prandtl Number(Pr)	0.7146
Length of the airfoil (L)	28 m

The next figure represent a section of the front of an airfoil with a piccolo tube inside.

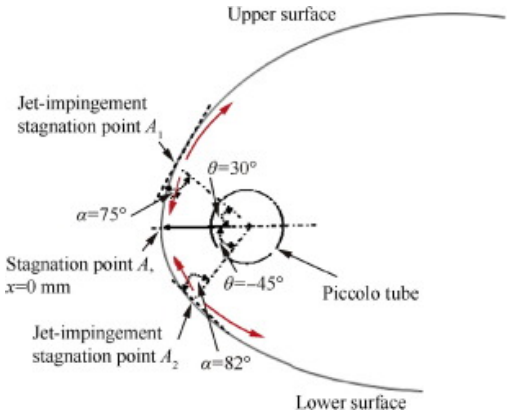

Figure 27: PICCOLO TUBE

The local heat transfer coefficient from the bleed air inside the airfoil can be calculated by using the Nusselt number correlation. The Nusselt number is a function of the Reynolds and Prandtl numbers in relation to the jet's geometric shape. Piccolo tubes heat the interior of the affected surfaces with an array of small hot air jets generated by this tube. The next equation is obtained with 3 rows of holes for the Nusselt number at the stagnation point.

$$Nu_d = \frac{hd}{k} = 1.827x10^{-4} Re_j^{1.1240.847}{}_{jet} (\frac{z_{jet}}{d_{jet}})^{-0.487} \tag{83}$$

The stagnation point is aligned with the holes and the leading edge. From here it is needed to make some assumption: the velocity of the bleed air almost reaches the speed of sound. The bleed air expands the moment it goes out of the piccolo tube. The pressure of the air is at 1 atm. The density and volume stay constant. Moreover, as shown in the study realized by [BU, 2016], this formula works within these ranges.

Parameters	Range
Re_j	$50x10^3 - 90x10^3$
z_{jet}/d_{jet}	1.74 - 20
jet	66 - 90

With these values calculated, it is possible to calculate the mass flow rate. With the next equation:

$$\dot{m} = \frac{\dot{Q}}{C_p * (Tf - Ti)} \tag{84}$$

As this system, the heat flow warm one surface from another as convection, the next equation can be used.

$$\dot{Q}_{conv} = h * A_s * (T_{sur} - T_i) \tag{85}$$

Therefore we combine these last equations to get, ($T_i = T_{bleedair}$):

$$\dot{m} = \frac{h * A_s(T_{sur} - T_{bleedair})}{C_p(T_f - T_i)} \tag{86}$$

The optimal Reynolds number is $85.8x10^3$. The distance between holes is $C_n = 50$ mm.Also a greater angle shows a higher heat transfer coefficient. The value of z is unknown but z/d value is according to this Reynolds number optimal for 4,1. The jet hole diameter is d=2 mm.In this way all the variables are completed except for the h which remain unknown. Therefore this next equation is needed to finally calculate heat transfer coefficient (at stagnation point).

$$Nu_{stag} = \frac{h_{stag} * d}{k} \tag{87}$$

With this final equation the mass flow can be calculated for the two different temperatures of 400K and 800K because the factor that help us to determine the differences in mass flow is the specific heat of air.

$$\dot{m} = \frac{h * A_s}{C_p} \tag{88}$$

Some results can be seen in the next table.

Parameters	400K	800K
Re_j	$85.8X10^3$	$85.8X10^3$
Nu_{stag}	47.3	47.3
cp_{jet} $J/(kg.K)$	1008	1040.7
$A_s m^2$	1.25x10^{-5}	1.25x10^{-5}
$k(W/mK)$	0.029885	0.043238
$h_{stag}[W/m^2K]$	885.49	1022.6
$\dot{m}[kg/s]$	$1.09x10^{-5}$	$1.22x10^{-5}$

These results for the mass flow represent the mass flow that crosses through a jet hole. This needs to be multiplied by the number of holes which is is obtained Dividing the length of the wing for the distance between each jet hole and after that multiplied by 3. The result for this number is $1.012x10^3$. As a conclusion the mass flow is quite small which in reality would not be enough to keep the temperature in the airfoil, but probably this is due to the fact of possible wrong calculations because this system is one of the most used around the world.

4 Design and analysis of an anti-icing system

4.1 Analysis of ice-phobic materials

To analyse whether an ice-phobic material on a wing could prevent ice forming on the wing the shear stress exerted by the boundary layer has to be calculated. To do this some assumptions have to be made.The surface of the plane is assumed to be a flat plate with an incompressible and steady-state flow with a linear velocity within the boundary layer. Further the pressure is assumed to be constant across the boundary layer.

$$\tau_w = C_f \frac{1}{2} \rho U^2 \tag{89}$$

With the friction coefficient dependant on the Reynolds number, for the dimension of the Reynolds number the mean aerodynamic chord is used to find the Reynolds number of the wing.

$$C_f = \frac{0.644}{\sqrt{Re}} \quad with \quad Re = \frac{UL}{\upsilon} \tag{90}$$

Parameter	Description	Value
ρ	Air density	1.276 kg/m^3
U	Free stream velocity	136.33 m/s
L	Mean aerodynamic chord	3.96m
υ	Kinematic viscosity of	13.49*10$^-$6 m^2/s

Table 7: Constants for formula 89

The found shear stress is 1.2071 pa, this is lower than the found ice adhesion strength which is around 20 kPa for a passive system. This means that the shear force in not strong enough to remove the ice on the wing, so an ice-phobic material alone is not a suitable solution to prevent ice accretion. An ice-phobic material can contribute in a hybrid system. The hydro-phobic component of an ice-phobic material causes droplets to easily move over the wing, reducing the time a droplet has to freeze, further the ice formation temperature is lowered because small air pockets are captured underneath the droplet which forms a good thermal insulation layer toe prevent freezing [31]. This is an advantage to prevent runback icing [32]. The droplets of ice that is melted at the front of the wing will move along the wing, these droplets can freeze along this path. With ice-phobic material this amount is reduced.

4.2 Design and optimisation anti-icing system

Optimizing impinging jets In this section, the jet diameter and the arrangement of the holes in span wise direction is optimised for a fully-evaporative system. Data obtained from 2D foil ice is to be compared with experimental data from "Jet impingement heat transfer on a concave surface in a wing leading edge: Experimental study and correlation development".

4.2.1 Optimizing of the jet diameter

In this process the Nusselt number required along chord wise direction is going to be compared with the Nusselt number impinging jets can provide for diferent diameters . First of all, the heat flux q_{req} as function of $\frac{(s_{stag}-s)}{c}$ distribution calculated with 2DFOIL-ICE. This function must be transormed a units comparable to the experiments,thus to Nu_{req} as function of $\frac{x}{d}$ In order to calculate Nu_{req}, the heat transfer coefficient required needs to be obtained first h_{req}. To find this last one, the next equation should be used.

$$h_{req}(s) = \frac{q_{req}(s)}{T_{air} - T_{sur}} \tag{91}$$

Where ($T_{air} = 400K$) is the temperature of the bleed air and ($Ts_{avg} = 300K$) the average temperature of the surface.

Then the function is converted to the required Nusselt number, in order to make this transformation the next equation is used.

$$Nu_{req} = \frac{h_{req}(d)}{k} \tag{92}$$

It is worth to be noted that the x-axis is not in the appropiate units so the following equation is used:

$$\frac{s - s_{stag} * (c)}{c * d} = \frac{x}{d} \tag{93}$$

The following graph presents the result from experiments conducted by Ramenzapour et al.

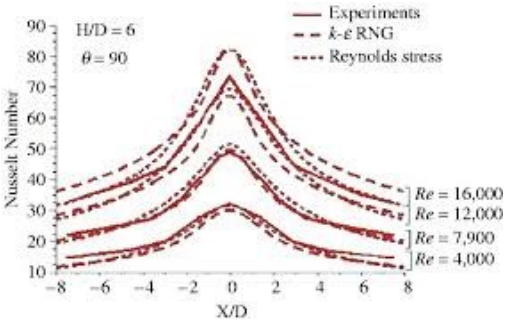

Figure 28: Experiment with different Reynolds numbers

The variable L is the tube-to-surface distance and D the diameter of the jet. In this case the ratio with value 6 is chosen because is beneficial to the designed system. The higher the Nusselt number the higher the maximum heat transfer. Under this reasoning the curve with the highest peak was chosen, the one that belongs to a Reynolds Number of 16000. The curve was approximated in MatLab using polyfit.

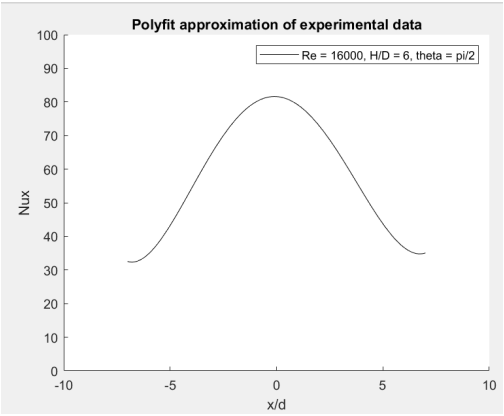

Figure 29: POLYFIT

Three different diammeters of jet holes are tested namely 2,5 qnd 8 mm. It is noticeable that the Local Nusselt number changes for each graph. The objective is to mantain it under the available Nusselt number of the jet. On the other hand, exaggerate peaks of provided Nusselt over the required one is not desirable. Note that the diameter configuration that fits the best is the one for two milimiters given that Nu_{jet} has just a slightly higher value than $Nureq$.

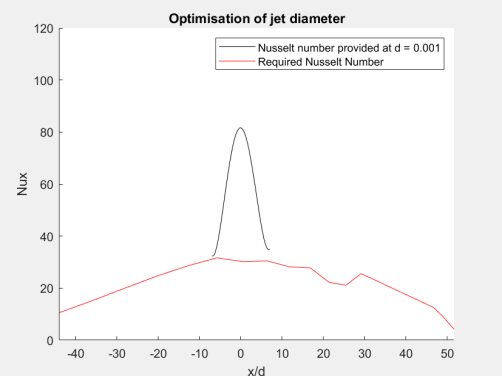

Figure 30: Diameter 1mm

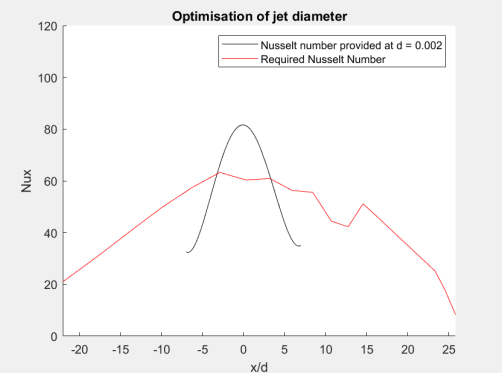

Figure 31: Diameter 2mm

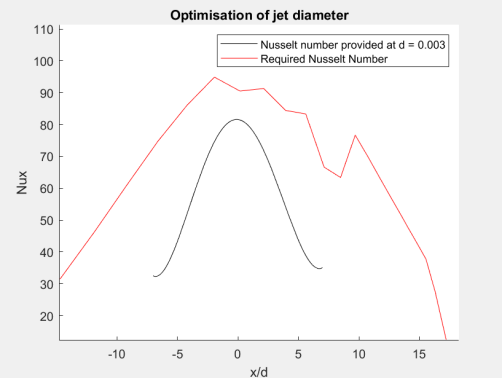

Figure 32: Diameter 3mm

As 2 mm diameter as the most suitable, the tube-to-surface distance can also be determined with the given relation.

$$\frac{H}{D} = 6 \tag{94}$$

Thus the final tube-to-surface distance would be 1.2 cm. From these results one can also conclude that one hole is not enough, 2 more rows of piccolo tubes should be added up and down and equally distant to the original. That translated to the graph means the addition of two identical curves to the plot. Similarly, this approach will be used to optimise the distribution of holes in span wise direction in the next section.

4.2.2 Optimizing of the jet diameter

As part of the impinging jet system optimisation, the distance between holes in y-direction, span wise, is determined. To perform this analysis, the maximum Nusselt number required closed to the stagnation point was collected from the Local Nusselt number as function of x/d from the previous section. This value was assumed to be constant along the wing span, that is why it is represented as a constant function in the graph below.

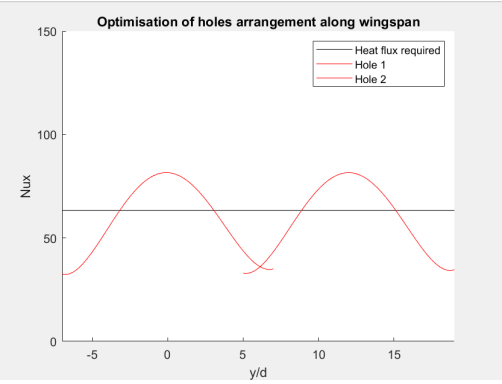

Figure 33: Optimization of holes along wingspan

The objective was to find an appropriate non dimensionless distance between two Local jet Nusselt number curves while covering the Nusselt number requirement. The area of required Nusselt number placed above the these two curves, is assumed to still be supplied by the required heat flux by the overlap of the curves below it. The dimensionless distance between these curves center-lines is 12.Therefore the distance between holes knowing their diameter (2 mm calculated in the previous section) is 2.4 cm. This value comes across as rather small and that could be the case. This is because, the experimental data used to optimised do not relate with the intrinsic characteristics of the system. For instance, the Reynolds Number was arbitrarily chosen to define the selected curve in the previous section. These not properly sustained assumptions create uncertainties about the reliability of the optimisation.

4.3 Evaluation of resulting temperature distribution

Once the analysis of every system has been done, this part will implement numerical calculations to evaluate the resulting temperature distribution first in the walls of the wing and second along the wing cross section. As most of the systems investigated were discarded, two of the systems most commonly used as anti icing systems will be taken into account; Electric heating mats and Impinging jets anti-icing systems.

4.3.1 Temperature distribution in the walls of the wing

Heating mats analysis

To start the analysis, it is necessary to adapt the existent equations to the actual problem. It is taken as reference the book [23], in which the heat conduction equations are given for different shapes. the walls of the wing are taken to be two concentric cylinders and the space between these is the wall thickness. The heat conduction equation for cylinders is given as follows,

$$\frac{1}{r}\frac{\delta}{\delta r}(kr\frac{\delta T}{\delta r}) + \frac{1}{r^2}\frac{\delta}{\delta \phi}(k\frac{\delta T}{\delta \phi}) + \frac{\delta}{\delta z}(k\frac{\delta T}{\delta z}) + \dot{e}_{gen} = \rho c\frac{\delta T}{\delta t} \tag{95}$$

As the analysis is done in 1D, only radius is considered and for better guide, Fig.25 show the model in a clearer way. Heat generation is neglected from the equation and it is considered to be steady-state. Thus the following reduced equation is obtained,

$$\frac{\delta}{\delta r}(kr\frac{\delta T}{\delta r}) = 0 \tag{96}$$

After solving the equation,

$$\frac{\delta T}{\delta r} = \frac{C_1}{r} \tag{97}$$

$$T(r) = C_1 \ln(r) + C_2 \tag{98}$$

The following boundary conditions are used: Constant temperature at the inner surface T_i, $T(R1) = T_i$. Also, constant flux at the inner surface $\dot{q}_r$, $\dot{q}_r = -k\frac{\delta T}{\delta r}|r = R1$.

Then the constants C_1 and C_2 are found using the boundary conditions above, given the temperature profile below.

$$T(r) = \frac{\dot{q}_r}{k} R_1(\ln(R_1) - \ln(r)) + T_i \tag{99}$$

The following data of heating mats is given in section 5.1, R1 = 0.3 m, R2 = 0.34 m, q = 530.5 W/m^2, T_i = 294.1 K, k = 205 W/mK. A graph of the temperature distribution as function of the radius is given below.

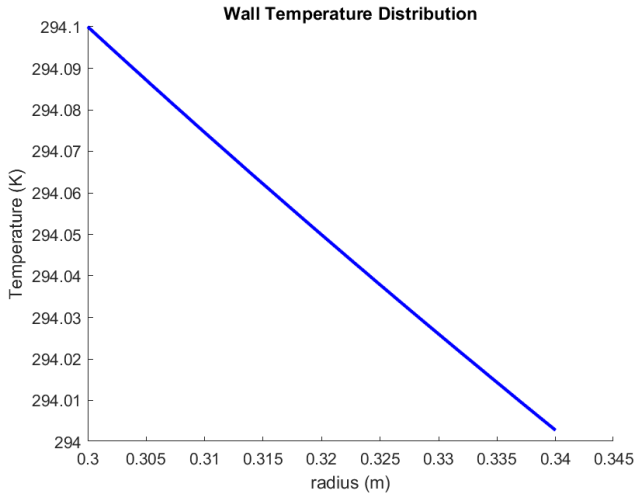

Figure 34: Temperature distribution in the walls using heating mats

Impinging jets analysis

For the next system, the same process is going to be implemented taken into account the same model of two concentric cylinders, equation is given below,

$$\frac{\delta T}{\delta r} = \frac{C_1}{r} \tag{100}$$

$$T(r) = C_1 \ln(r) + C_2 \tag{101}$$

The following boundary conditions are used: Constant temperature at the outer surface T_s, $T(R2) = T_s$. Also, constant flux at the outer surface $\dot{q}_r$, $\dot{q}_r = -k\frac{\delta T}{\delta r}|r = R2$.

Then the constants C_1 and C_2 are found using the boundary conditions above, given the temperature profile below.

$$T(r) = \frac{\dot{q}_r}{k} R_2(\ln(R2) - \ln(r)) + T_s \tag{102}$$

The heat flux delivered by the impinging jets system was calculated based in the temperature of the bleed air given in part 5.4 and the temperature needed for de-icing given by 2DFOIL-ICE, the radius difference between the tube carrying the bleed air and the leading edge. The equation and corresponding result are given below

$$\dot{q} = \frac{kR2(T_i - T_s)}{\ln(\frac{R2}{R1})} = 12.5kW/m^2 \tag{103}$$

The following data of impinging jets is given in section 5.4, R1 = 0.18 m, R2 = 0.34 m, T_s = 310 K, T_i = 424 K, k = 205 W/mK. A graph of the temperature distribution as function of the radius is given below.

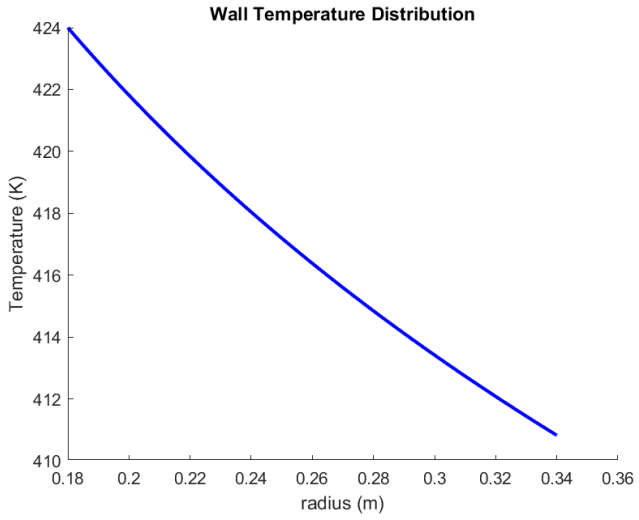

Figure 35: Temperature distribution in the walls using impinging jets

4.3.2 Temperature distribution along wing cross-section

Heating mats analysis In order to get the temperature distribution along the wing cross section, a cut will be done parallel and in the middle of the wing, so the heat conduction equation could be analyzed as a cube but only taken into account 1D. From the top view of the cube, a plate will be seen divided by a line which symbolizes the anti-icing system, the left part represent the leading edge and the right part the trailing edge of the wing. For a better perspective of the model see Fig 36 in which distances are also detailed.

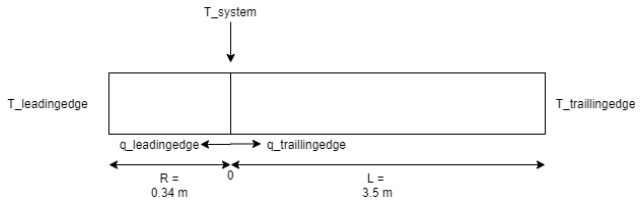

Figure 36: Representation of the cross section of the wing showing leading edge and trailing edge

The following equation is given according to [23] for a cube geometry,

$$\frac{\delta}{\delta x}(k\frac{\delta T}{\delta x}) + \frac{\delta}{\delta y}(k\frac{\delta T}{\delta y}) + \frac{\delta}{\delta z}(k\frac{\delta T}{\delta z}) + \dot{e}_{gen} = \rho c\frac{\delta T}{\delta t} \tag{104}$$

Steady-state and no heat generation system is again considered en therefore the equation is simplified to,

$$\frac{\delta}{\delta x}(k\frac{\delta T}{\delta x}) = 0 \tag{105}$$

Solving the equation, it is obtained:

$$\frac{\delta T}{\delta x} = C_1 \tag{106}$$

$$T(x) = C_1 x + C_2 \tag{107}$$

The following boundary conditions are used for the left plate: Temperature of the heating mats $T_{heatingmats} = 294.1K$ and a constant heat flux $\dot{q}_{leadingedge} = 530.5W/m^2$ calculated for heating mats. The following equation is used,

$$T(x) = \frac{-\dot{q}}{k}x + T_{heatingmats} \tag{108}$$

And for the right plate:The temperature of the trailing edge being set according to the worst case temperature in which ice accretes which is chosen to be $T_{trailingedge} = 263K$ according to the literature study part and a constant heat flux of $\dot{q}_{trailingedge} = 1.82kW/m^2$. The same boundary conditions of the left plate are taken but in the opposite direction, therefore opposite sign. Resulting in.

$$T(x) = \frac{\dot{q}}{k}x + T_{heatingmats} \tag{109}$$

The graph below shows the temperature distribution.

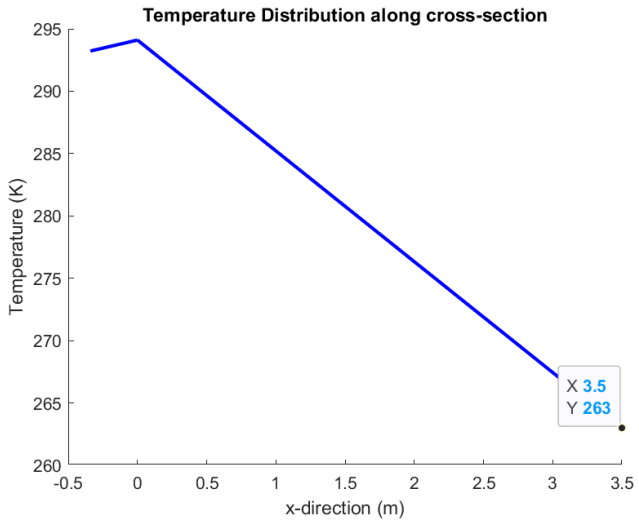

Figure 37: Temperature distribution along cross-section using heating mats

Impinging jets analysis

Now for the Impinging jets analysis, the same model as before is used and therefore the equations used are the same, steady-state and no heat generation system is considered,

$$\frac{\delta T}{\delta x} = C_1 \tag{110}$$

$$T(x) = C_1 x + C_2 \tag{111}$$

The following boundary conditions are used for the left plate: Temperature of the impinging jets $T_{impingingjets} = 424K$ and a constant heat flux $\dot{q}_{leadingedge} = 12.5kW/m^2$ calculated for impinging jets. The following equation is used,

$$T(x) = \frac{-\dot{q}}{k}x + T_{impingingjets} \tag{112}$$

And for the right plate:The temperature of the trailing edge being set according to the worst case temperature in which ice accretes which is chosen to be $T_{trailingedge} = 263K$ according to the literature study part and a constant heat flux of $\dot{q}_{trailingedge} = 9.4kW/m^2$. The same boundary conditions of the left plate are taken but in the opposite direction, therefore opposite sign. Resulting in.

$$T(x) = \frac{\dot{q}}{k}x + T_{impingingjets} \tag{113}$$

The graph below shows the temperature distribution.

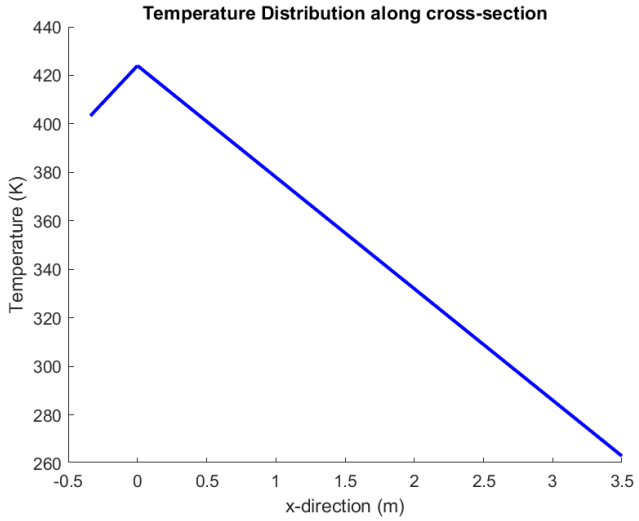

Figure 38: Temperature distribution along cross-section using impinging jets

5 Ethics

5.1 Introduction to ethics

For the new Boeing 737-800 commercial aircraft Boeing management contracted an engineering team to design the anti-icing system for the aircraft. After the design was finished Boeing management choose to use an already existing system instead with no redundancy in the icing sensors. Boeing tried to use software to make sure that the system is not blind if the sensor failed. Despite this the system cause several plane crashes which caused Boeing's stock to go down by 40 %.

5.2 Step 1

By choosing an already existing system over the newly designed one. Here was chosen for the cheapest option for the company, but because there is no redundancy in the icing sensors the safety of this system was reduced. It is clear that this was not safe so Being tried to improve the safety with specialized software. This choice endangers the lives of the passengers flying with the Boeing 737-800

Another risk imposed is that pilot can't fully trust their plane. Because the sensor where the anti-icing system relies on can't always be trusted.

On the business side also risk have been taken, with the choice to use a cheaper alternative to increase there profits. The result is that the stock of Boeing decreased by 40%. Because people don't trust the planes of Boeing any more and their reputation has decreased significantly, which will have an effect on the for a long time.

5.3 Step 2: Ethical Pre-mortems

While the previously explained risk-sweeping protocol only focusses on the individual risks, a pre-mortem analysis sets its focus on avoinding systematic ethical failures of a project. "Many ethical disasters in engineering and design have resulted from the cascade effect: multiple team failures that in isolation would not have jeopardized the project, but in concert produced aggregate ethical disaster"[33]. Using moral imagination, to predict which ethical failures might easily happen, and take notes of the preventable causes, so that the disaster can be minimized or avoided. Quiet global questions look like: 'how could this project fail for ethical reasons?'or 'what blind spots would lead us into it?'. This can lead to questions such as: "what systems/processes/checks/fail-safes can we incorporate in order to reduce the ethical failure risk?". Therefore a list of applicable question w.r.t. the new anti-icing system was setup and are listed down below:

- Have we prioritized the safety and well being of passengers and the working staff, above all other aspects such as company profits, and maybe thereby ignoring regulations for the sake of firm benefits. With others words, are there any (on purpose) overlooked safety measures?

- Did we rush and/or skip important design steps within the design process, such as highly extreme and unusual weather conditions calculations? Because of the new designed anti-icing system, the plane probably should undergo an appropriate resilience test instead of giving it the same aptitude test as previous models in order to save training time for the pilots and staff?

- Have we looked at all the separate working divisions, such as the engineering team and/or the software programmers? Making sure that there was no miscommunication between the employee levels. For example misjudging the importance of a component and over reliance on another due to decision making of the company management, and thereby disencouraging employees to express faults.

- Did we not let ourselves be guided too much by the urge of competing with other companies within the aviation branch? Prioritizing aspects other than safety and quality to achieve economic dominance. Overconfidence of the obtained changes.

- Did we respond with respect to aerodynamics and other conditions that are checked during test flights and compared with old models? Thereby gaining enough knowledge on how to train pilots and staff, or maybe retraining to distribute all information that covers the changes made to the airplane. Encouraging staff to give advice and opinions regarding safety of the new system and faults that still might be present.

- Does the newly designed anti-icing system completely align with the FAA regulations? Instead of making use of short cuts and loopholes within the legislation, and thereby overlooking the product safety and quality assurance.

The pre-mortem process is supported by an addition to the company onboarding process, in which employees are presented with an overview of the company's ethical values, culture, and processes; provided with a review and discussion of the distinctive ethical risks and concerns that emerge in airplane anti-icing design and development; given a conceptual framework and safety regulations for identifying such ethical concerns; and asked to review and discuss an ethical case study, such as the post-mortem of previous aircraft disasters.

5.4 Step 3

The goal of this stakeholder analysis is to gain valuable information and insights which are of interest for multi-purposes during the designing of the anti-icing system. First by means of gaining early alignment among all stakeholders on the goals and plans. This will contribute to ensuring that each stakeholder starts the project with a clear understanding what needs to be done, and how to contribute to achieve the pursued successful outcome. Secondly, an pre-project conducted stakeholder analysis identifies conflicts and issues in the begin phase. And lastly this gives clarity for determining which influencers, stakeholder and other key organizational players that are valuable to involve in/during the project. Enlisting these players in the begin phase will increase the likely hood of earning their support for the project, and thereby raising the chance to bring the project to a successful end.

From this it follows that a list of stakeholders has been composed. Afterwards these stakeholders have been categorised in terms of their influence, interest, and levels of participation in the project. The list of interest for the stakeholders is shown in Table. 8. The categorization for the interest is important to get an clear overview of which stakeholder shares the same interests.

Stakeholder	Interested in the impact					
	Finance	Environment	Reputation	Technology	Reliability	Legislation
Boeing	✓		✓	✓	✓	✓
Engineering Team		✓		✓	✓	
A.I. Team				✓	✓	
FAA		✓			✓	✓
Suppliers	✓					
Costumers						✓
Shareholder	✓					
Employees	✓		✓			
Pilot + Crew					✓	
Government		✓			✓	✓
Competitors			✓		✓	✓
Media	✓	✓			✓	✓
Passengers + families					✓	

Table 8: Interests in the impact list per stakeholder

The above stated stakeholders are divided within two subgroups namely, the primary and the secondary stakeholders. Within this division, these stakeholders are again sub-divided within internal stakeholders or external stakeholders. This is done to emphasize how each stakeholder is located in relation with Boeing. The stakeholders that are in direct contact with Boeing are classified within the internal stakeholders. The external stakeholders merely have a relationship with Boeing, instead of being in a position to participate and influence on the realization of the design process. This has been done by making a Power-Interest Chart, shown in Fig. 39b, and the group distribution as shown in Fig. 39a.

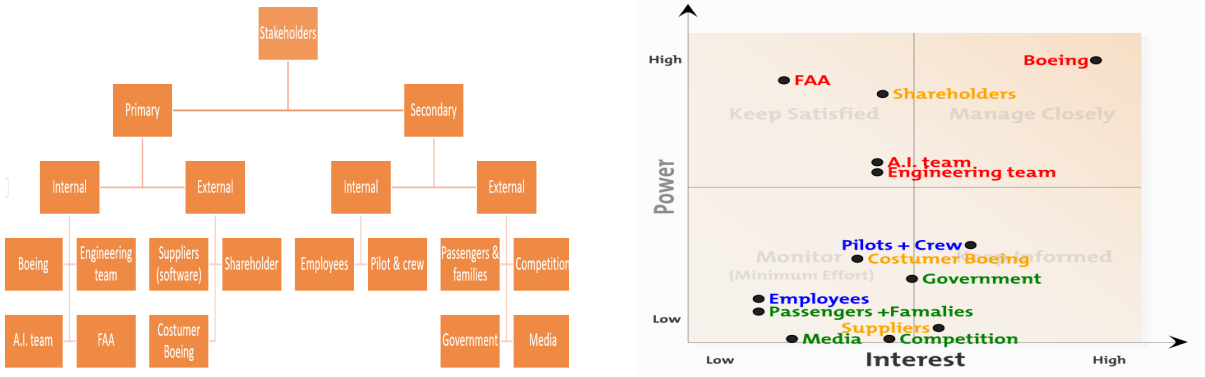

(a) Stakeholders map

(b) Stakeholders Power-Interest chart

Figure 39: Stakeholders overview

As can be seen from Fig. 39b, there is made a division of colours for all the stakeholders. This done to emphasis the stakeholder mapping as depicted in Fig. 39a.

- Red: Primary Internal Stakeholders.
- Orange: Primary External Stakeholders.
- Blue: Secondary Internal Stakeholders.

- Green: Secondary External Stakeholders.

5.5 Step 4 Case-based analyses

on February 12, 2012, Colgan air Flight 3407 was en route from Newark, New Jersey, to Buffalo, New York. The aircraft, a Bombardier Dash-8 Q400, entered into an aerodynamic stall. Unfortunately it did not recover and crashed into a house in Clarence Center, New York at 10.17 p.m., killing all 49 passengers and crew on board, as well as one person located inside the house.

The crash had several reasons, for which many different people can be blamed. There were already some similar crashes before, because of ice accretion on the wings. The crash of Flight 3407 was again caused by ice accretion on the wings, but this time the crash was caused by a second factor. The critical decisions taken by the pilot.

Because of earlier catastrophic crashes by ice accretion on wings, for example in October 1994 (American Eagle) and in January 1997 (Com Air) with the ATR72 plane, there were already major steps taken to avoid crashes by ice accretion. For example all the planes were now provided with an good anti-icing system. Another step taken was that all pilots were recommended to fly manually in icing conditions. In December 2008, the NTSB came out with a new recommendation for all pilots, because they issued the safety about the danger of keeping the autopilot engaged during icing conditions. Manually flying would be essential here, because this will ensure pilots to be able to detect changes in the handling characteristics of the airplane, which are a warning sign of ice accumulation.

On flight 3407 both things went wrong, with fatal consequences. First of all the anti-icing system did not work perfectly, because there was a lot of ice accretion on the wings of the airplane. Secondly, the pilot did not act in the way he had to act to the stick shaker stall warning, that directly will activate the stick pusher. As designed, this will push the nose down when it sensed a stall was imminent, but the pilot again reacted improperly and overrode that additional safety device by pulling back again on the control column, causing the plane to stall and this was one of the reasons of the fatal crash.

On May 11, 2009, information about the training record was released about the pilot of flight 3407. He had failed three important "check rides", so the investigators suggested that he might not have been adequately trained to respond to the emergency that led to the airplane's fatal descent.

This case is one of many airplane crashes, where many decisions done by different people, caused a fatal crash. Also from an ethical view, many things went wrong. For example Colgan, who let this pilot fly this plane, who did not have enough training to react on crucial moments like this. With many passengers in a plane, it is not very ethical to let a relatively low skilled pilot fly. Money can be a big reason for this, because when there are not enough pilots for a company, they have to choose between decrease the amount of flights or taken less trained pilots. The first option is more ethical, because there are just well trained pilot in the air. A disadvantage is that when there are less flights, the flights are also more expensive. The second option is less ethical. Taken these less trained pilots in your company is a risk, but the prices of flights can stay lower and the company can be more profitable. These kind of decisions are always very difficult to take. After this crash new rules were introduced in the United States to let decisions like this never cause a fatal crash anymore.

[34]

5.6 Step 5: Ethical benefits of creative work

Boeing is one of the leaders in the aircraft manufacturing industry. To stay on top of this business it is always important to be an innovative company, otherwise this leading place can come in danger. In 2017, Boeing created a new 737 version, the 737-MAX. The biggest innovation of this new 737-type was that this airplane had a larger engine then the ones before, but the problem was that it was not entirely compatible. The changes done had for example some negatively impacts on the aerodynamics and instead of redesigning the airframe, they created some software updates. However, pilots who were flying a 737 were just never

informed about the new software system, which resulted in multiple crashes.

To remember ethical benefits of creative work it is important to understand why companies make these kind of decisions and for what good ends. It is even a question if the society is really better off with this innovations. Another important thing to realise is what we are willing to sacrifice to do everything right.

As mentioned before, it is really important for companies to stay innovative. When a company makes new updates, this will always cost a lot of money. Still they want to spend the least money possible on for example the manufacturing costs to maximize the profits and to let the price of the flights as low as possible. Here remember to look carefully at the ethical benefits, because these reasons would only be justified if it does not result in many crashes. One of the biggest problems is that the companies are constantly under big pressure to develop new innovations and when they figure out some small problems they prefer to fix it fast and cheap using some software updates if possible instead of redesigning parts. Looking at the anti-icing system, Boeing wants to use the cheapest system possible. Off course it has to be safe, but also here, money is a very important factor. Spending more money to be 100% sure it is a safe system or spending less money with a small change of failure of the system.

To figure out if the society is better of with this innovations, the risks have to be analysed. Lower costs for manufacturing processes can for example be more profitable for customers (lower flight prices), but how much risk does for example Boeing wants to take for this lower prices. Instead of lowering flight prices, they could also use the profits to give better training to their pilots or for even better research for future updates for for example an improved anti-icing system. So it is very important to find a good balance between costs and safety.

Realising what we are willing to sacrifice to do everything right is a difficult part. Money is again the most important factor. Off course Boeing tries as much as possible to build very safe planes, but they never spend more money then necessary. When for a specific anti-icing system one sensor is enough, they normally do not place an extra sensor for extra safety. It is also very easy to accuse Boeing for unethical behaviour, but aircraft manufacturing is still a volatile business and also these companies have to remain profitable.

When looking at the ethical benefits of creative works it remains difficult. At one side customers want the planes as safe as possible, but at the other side do not want to pay to much for a plane ticket. Plane manufacturing companies try to be as innovative as possible and try to build as safe planes as possible, but do not want to spend more money then necessary, to stay profitable.

5.7 Step 6: Thinking about terrible people

The idea behind this ethical tool is that inventions are not always used as they are intended. It must be considered that some people will try to gain benefit from it hurting others in the process. Other people could use them with alarming irrationality, being a threat to themselves or the others. Part of the job of a designer is to foresee the danger and reduce the chances of it to happen. Gather critical information of similar apparatus that already interact with consumers may give some guidance to where to direct the exercise.

The following section will apply this tool to the anti-icing method designed in this report. The first question that should be asked is: Who will want to abuse, steal, misinterpret, hack, destroy, or weaponize what we built? To answer this question, the possible aggressors can be divided into two groups: external and internal. Hackers fall into the former group while Boeing executives into the latter.

Hackers are one of the first concern that pops up when thinking on fully automotive system on which human lives relies. The latest aircraft computer systems have been developed upon this fundamental pillar but 90% of the commercial planes do not have proper protections.[35]. Nowadays, only two cases of aircraft hacking have been documented, committed by “white hat hackers” with academic and security purposes. In both scenarios, the researchers “only” got access to the radio communication systems or Wi-fi router on the plane. The avionics systems, the one that controls the critical equipment for navigation and motion, is completely sealed to the rest of the airplane. Even though these events are not surprising nor worrying for some experts, they show the growing hacking vulnerability of aircraft systems now. Thus, an automatic anti-icing system

must be developed with cyber security present all the time.

Internal aggressors are easily overlooked and that is why they play a dramatic role. One example of this problematic is the 737 Boeing max case. This was an example of a series of bad engineering and management decisions to reduce cost. [36], pilot and software developer claims that Boeing tried to solve hardware issues with software implementation. The 737-max showed visible aerodynamic issues due to engine and wingspan modifications. The company tried to tackle this issue by adding a fully automatic system that controls the plane when a critical angle of attack is given by a sensor. Only one sensor was placed on the nose of the plane, this makes the system too 'rigid' since a failure of this input collector represents a failure for the whole system. Another error in the design was letting the system take over the airplane in critical situation while ignoring any order given in the control cabin.

The next question that should be: Who will use it with alarming stupidity or irrationality? It should be note that internal aggressor can be classified into this group arguing that their actions are excused by a lack of training or simply ignorance. However, in the previous question it was assumed that their actions were premeditated, and the risk foreseen but ignored. Negligent pilots are who mainly composed this group. There is no doubt that commercial aircraft pilots receive a big amount of training, but human error can not be neglected during the design phase. Some factor may affect pilot's performance and quality of decision making. Alcohol is one of them and although it is not very frequently, there are reported cases of pilot that tried to start their journey over the legal alcohol limit. In fact, between, 2010 and 2019 177,000 pilots were tested and 99 were found above the legal limit. [37]. Besides alcohol, tiredness result of long journey also is present which may present in similar effects.

Even though the previous mentioned factor should be considered in the design phase. They are not particularly relevant to a automatic anti-icing system. Pilots that commit to fly an airplane with not enough training, relying solely on the autonomy of the system. If something goes wrong, they would not be able to make the proper decisions. For a designer it is hard to be involved in the regulations of training for flight staff so they should expect the worst can happen sometime. The manual control of the anti-system, when required, should be intuitive and alike currently used systems.

What rewards/incentives/openings has our design inadvertently created for those people? For this question, internal aggressor will be examined since they respond more adequately to our case. This is a positive trait, but it also can encourage its misuse. Similarly, to Boeing incidents, the software for anti-icing system can be used to reduce costs by fixing pre-existent hardware problems because installing software is cheaper than modifying the aerodynamic of hundreds of airplanes.

How can we remove those rewards/incentives? The design of an automatic anti-icing system should not only follow the guidelines for cybersecurity but also redundancy engineering. This means that multiple anti-icing sensors must be implemented. Additionally, experienced pilots should be involved during the whole process of design to avoid bubble mentality in the team. According to [36], pilots not only take input from one sensor but rely on many others that at first glance, might not be even related for a non-expert.

In conclusion, a newly implemented software shall not be as the only piece that keeps the plane together but as a part of a functional and properly design machine that can still work if any of its pieces fail. It is challenging for designers to assure their creations will not be abused by their own employer. Governmental authorities must control with more detail minimal safety measures of all the products that reach the market, especially those which can represent risk of life.

5.8 Step 7: Closing the Feedback Loops

The feedback loop is a tool used to effectively change the human behavior. The feedback loop is part of a system where the outputs or data collected from a measurable system are input for future operations.To better understanding, the elements and stages are going to be explained.

The elements of the feedback loop are: the receptor which is the sensory organ; the stimulus which is an action that evokes a response; the effector is an organ that acts in response and finally the response is the

cause action of the effector. Moreover, this system also has four stages: the evidence stage which is the responsible to collect the data; the relevance stage, where the information is relayed to the individual. The consequence stage, which is required to illuminate more paths ahead; the action stage where the individual take action and re-calibrate the behavior.

Once explained the concept of a feedback loop it is needed to adapt this system to our case, to the anti-icing system designed in this project. In order to success with this design is needed to understand that ethical design is never a finished task. With this thinking, the company will improve their statutes offering more capitations to the pilots and technical group workers to understand the new mechanisms developed. In addition to this,team groups of different areas must work proactively improving the workflow of throughout the company.

Once this is achieved is necessary to identify the feedback channels, as a consequence, hierarchy chains are created in case of any accident is presented regarding the new updates. One council called 'risk analysis and management' is created to evaluate the possible risks that it could experiment. These problems and future solutions are communicated by the person in charge of that group to the general management where its approbation would be required to further re-designing. This leads to the integration of the process and quality management. The company makes emphasis on the redundant engineering every time a new updated is required. In this way not just one sensor would be implemented, as the case of the Boeing 737-800 max, but 2 or more in case of needed. Offering in this way to the pilots, different data collected to act accordingly the situation.

After this process that is repeated every time a risk is analysed and a new solution is implemented. The design has reached its maximum optimal work confirming the lowest risk percentage. The general management presents the new design to another evaluator as, the FAA or the government to receive external approbation that the system is safe for the people. This complete process which is carried out by the company helps to gain reliability trough the different users and companies that buy the new updates. This will increase the sales of the company which will have more resources to continue implementing more procedures to close the feedback loop.

As a conclusion the company will "make a name" meaning responsibility and compromise with the safety of the users and investors. Due to the new policy applied in the company where safety will mean more incomes. Moreover, with the proactive work between different sub groups of the company the bubble mentality is "broken". In addition to this, the new hierarchy chains created would enhance the work and response in case of any accident. As a pre-mort case this would be the procedure to be carried out in the company in order to make the design of the anti-icing system.

6 Discussion

7 Conclusions

After the analysis of different aircraft anti-icing systems for the Boeing 737, the following conclusions are made:

- From the 2DFOIL ICE analysis, follows that for the most critical icing situation the required heat is 6.78 kW/m2. This is for a fully evaporative anti-icing system.

- The most critical condition for which the analysis was done in 2DFOIL ICE was the holding situation. The conditions for this state are a MVD of 20 µm and a LWC value of 1.70 g/m3. The most critical condition occurs at -20°and an altitude of 17747 ft. In this critical situation the angle of attack is 2.3°and the speed is 136.33 m/s.

- Depending on different air speeds, altitudes, temperatures and MVDs, the unprotected airfoil experiences a mix of rime and glaze ice, mostly around the leading edge of the airplane wing. The fully evaporative anti-icing system heats an area around the stagnation point of the wing. This keeps the wing completely free of ice.

- Regarding the possible anti-icing systems, detailed calculations showed different results for the different anti-icing systems analyzed, radiation and natural convection heat transfer couldnt deliver enough heat in order to reach the necessary temperature given by 2DFOIL-ICE and de-ice the surface of the wing with the most risk of ice catching which is the leading edge, for these two heat transfer types the models analyzed were for two concentric cylinders and therefore the formulas used correspond to this model.

- The shear stress of the boundary layer is not strong enough to remove ice on the wing. An ice-phobic material could be used in an hybrid system.

A Tables and figures

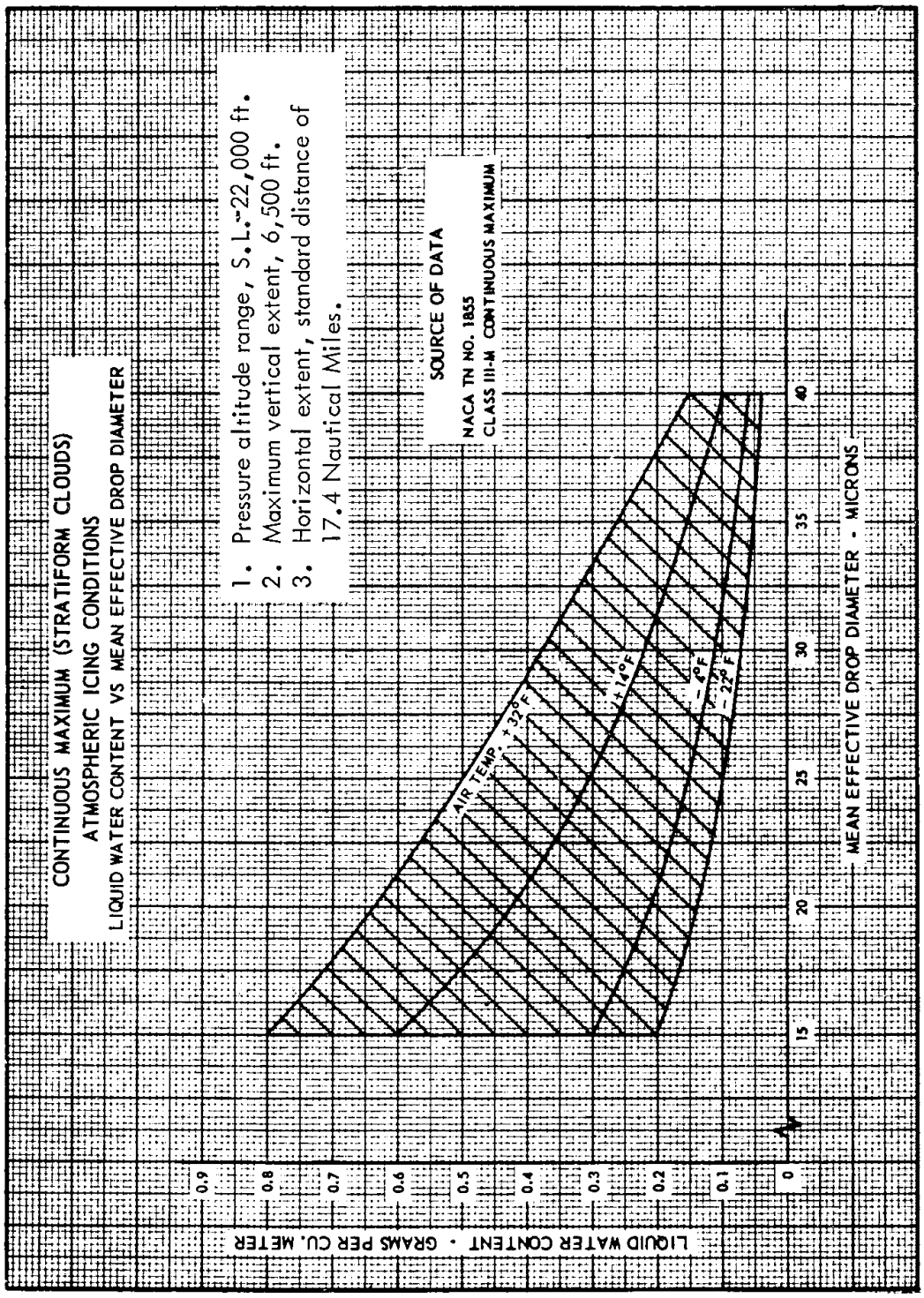

Figure 40: Variables of the cloud liquid water content, the mean effective diameter of the cloud droplets, the ambient air temperature and the interrelationship of these three variables (CM)

FIGURE 2

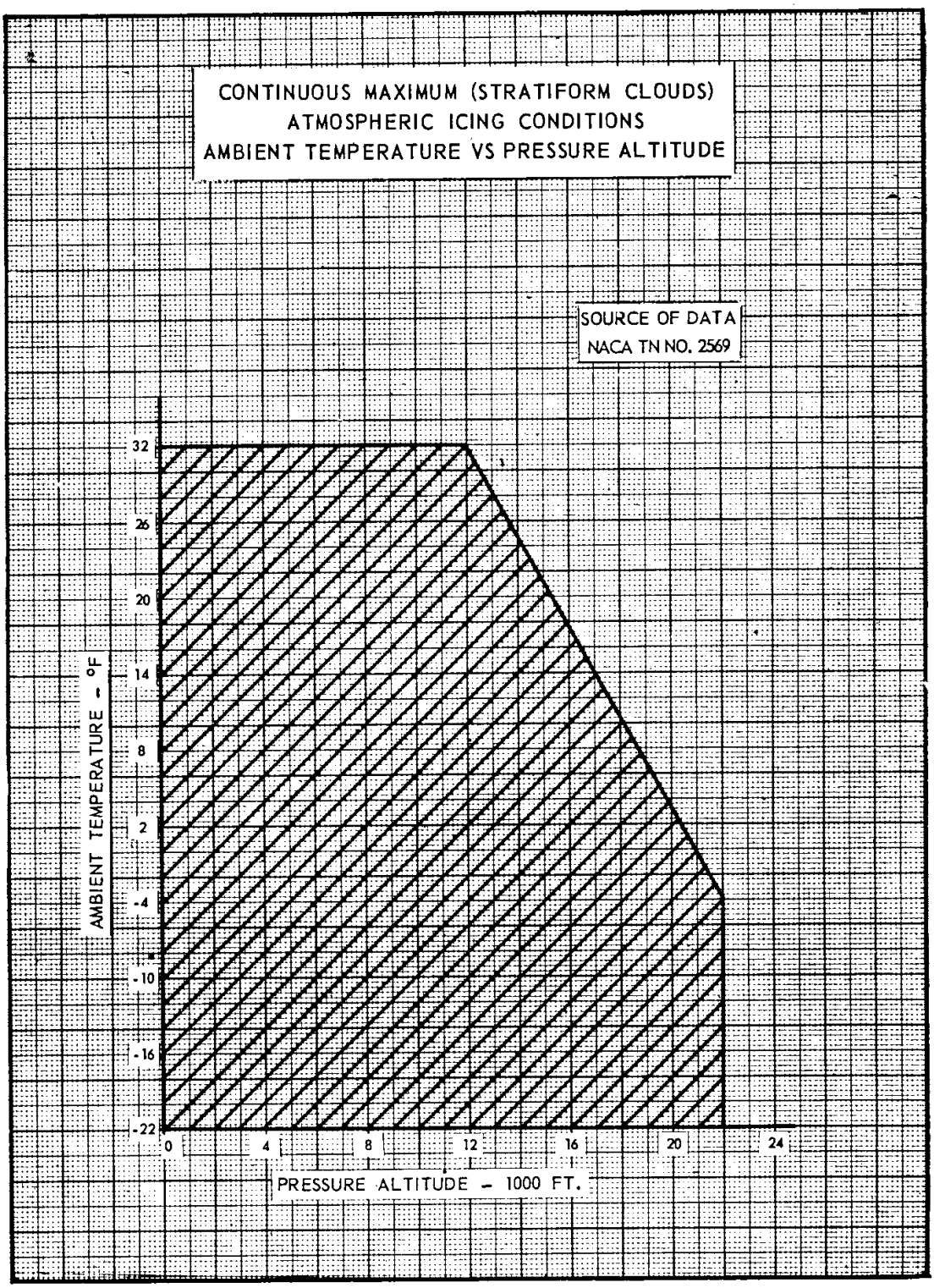

Figure 41: The limiting icing envelope in terms of altitude and temperature (CM)

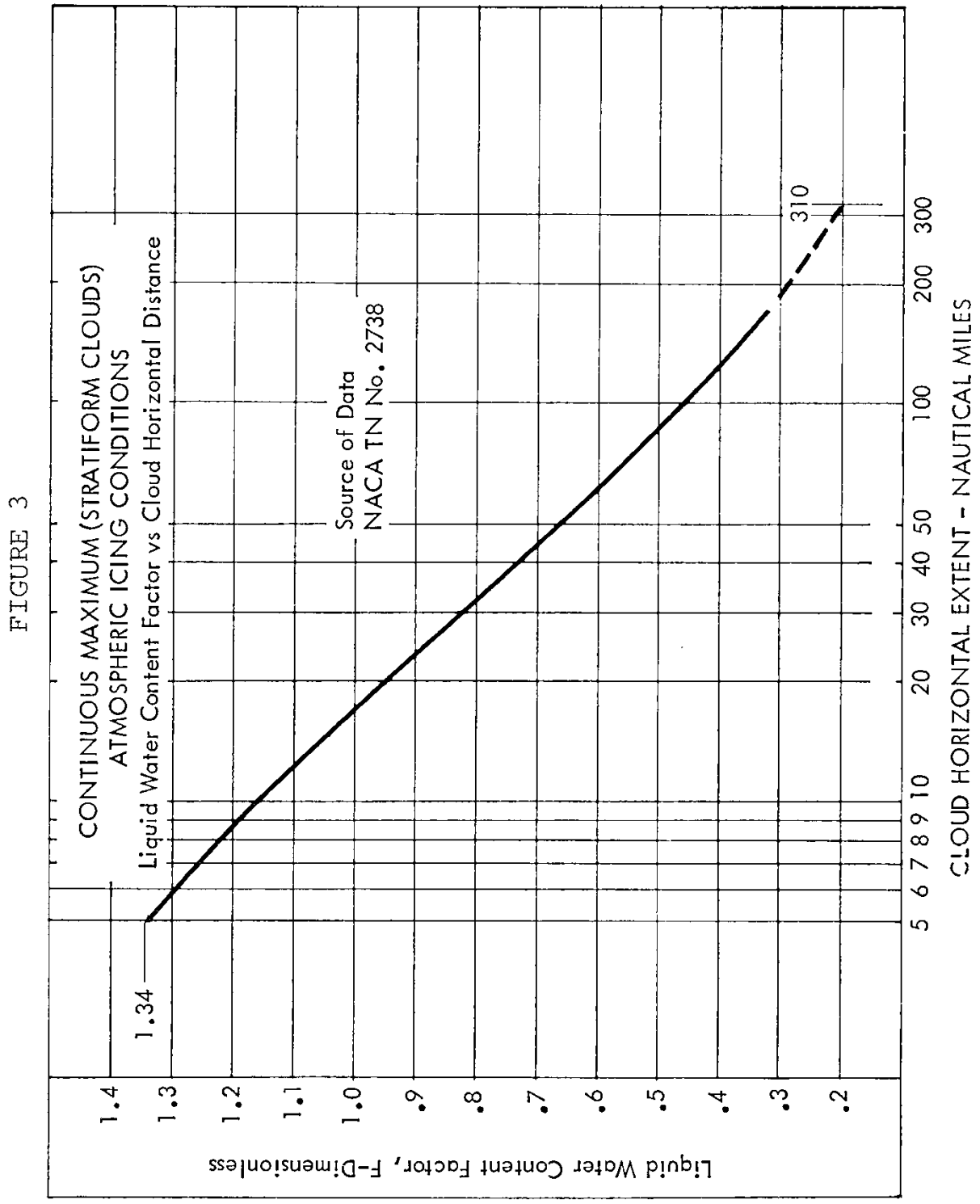

Figure 42: Liquid water content factors (CM)

FIGURE 4

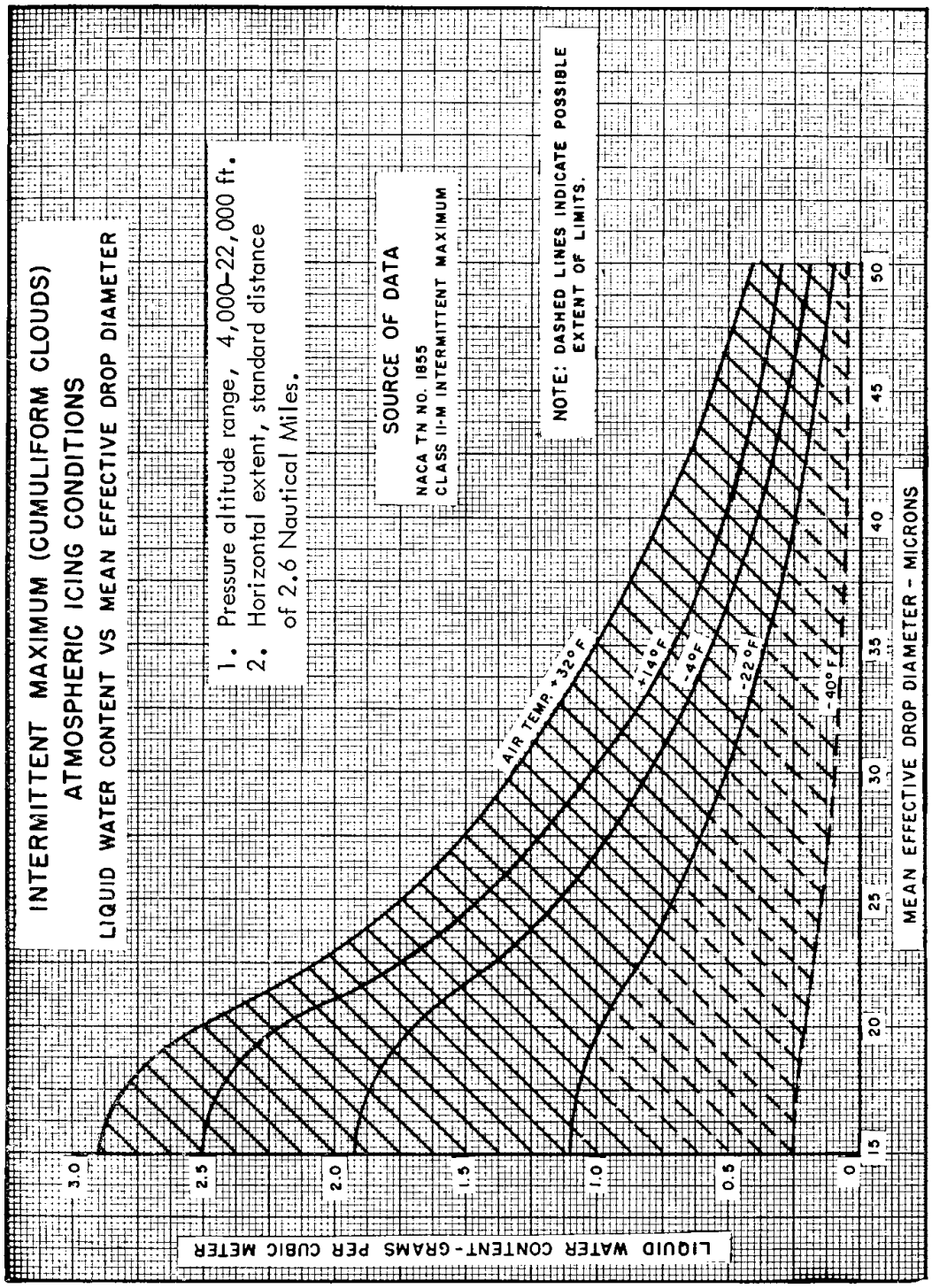

Figure 43: Variables of the cloud liquid water content, the mean effective diameter of the cloud droplets, the ambient air temperature and the interrelationship of these three variables (IM)

FIGURE 5

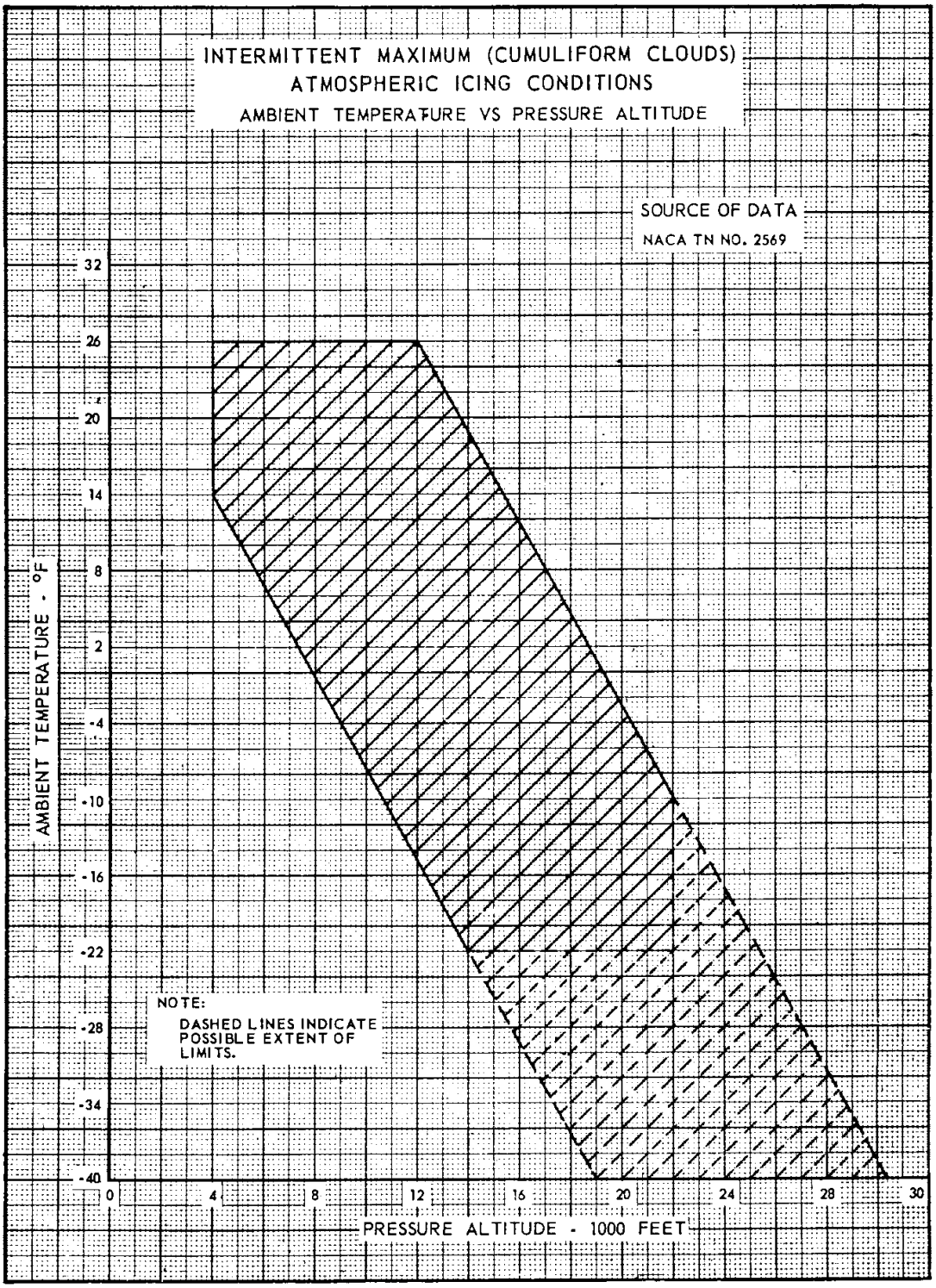

Figure 44: The limiting icing envelope in terms of altitude and temperature (IM)

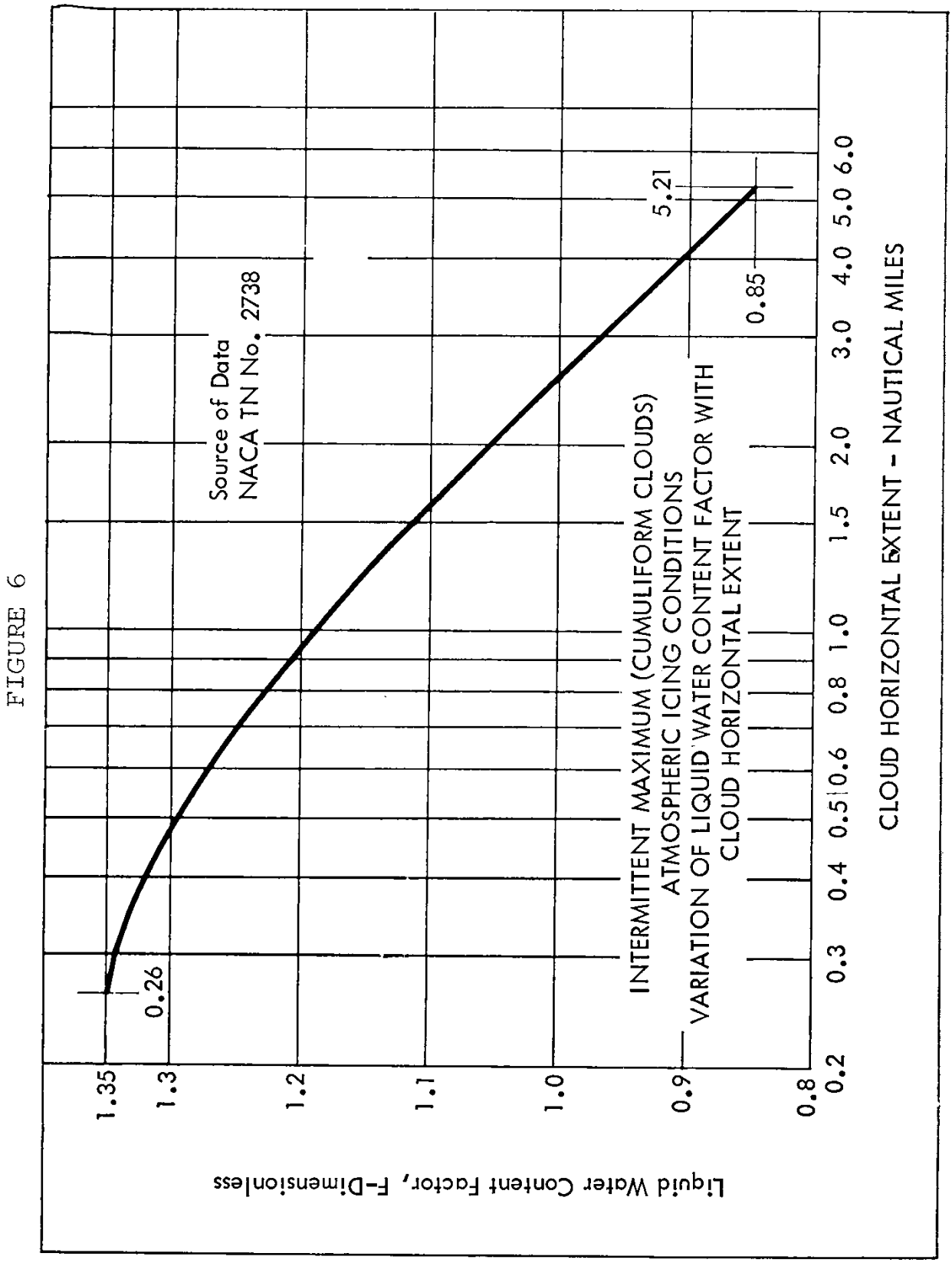

Figure 45: Liquid water content factors (IM)

ALTITUDE (Feet)	TEMP. (°C)	PRESSURE			PRESSURE RATIO $\delta = P/Po$	DENSITY $\sigma = \rho/\rho o$	Speed of sound (kt)	ALTITUDE (meters)
		hPa	PSI	In.Hg				
40 000	- 56.5	188	2.72	5.54	0.1851	0.2462	573	12 192
39 000	- 56.5	197	2.58	5.81	0.1942	0.2583	573	11 887
38 000	- 56.5	206	2.99	6.10	0.2038	0.2710	573	11 582
37 000	- 56.5	217	3.14	6.40	0.2138	0.2844	573	11 278
36 000	- 56.3	227	3.30	6.71	0.2243	0.2981	573	10 973
35 000	- 54.3	238	3.46	7.04	0.2353	0.3099	576	10 668
34 000	- 52.4	250	3.63	7.38	0.2467	0.3220	579	10 363
33 000	- 50.4	262	3.80	7.74	0.2586	0.3345	581	10 058
32 000	- 48.4	274	3.98	8.11	0.2709	0.3473	584	9 754
31 000	- 46.4	287	4.17	8.49	0.2837	0.3605	586	9 449
30 000	- 44.4	301	4.36	8.89	0.2970	0.3741	589	9 144
29 000	- 42.5	315	4.57	9.30	0.3107	0.3881	591	8 839
28 000	- 40.5	329	4.78	9.73	0.3250	0.4025	594	8 534
27 000	- 38.5	344	4.99	10.17	0.3398	0.4173	597	8 230
26 000	- 36.5	360	5.22	10.63	0.3552	0.4325	599	7 925
25 000	- 34.5	376	5.45	11.10	0.3711	0.4481	602	7 620
24 000	- 32.5	393	5.70	11.60	0.3876	0.4642	604	7 315
23 000	- 30.6	410	5.95	12.11	0.4046	0.4806	607	7 010
22 000	- 28.6	428	6.21	12.64	0.4223	0.4976	609	6 706
21 000	- 26.6	446	6.47	13.18	0.4406	0.5150	611	6 401
20 000	- 24.6	466	6.75	13.75	0.4595	0.5328	614	6 096
19 000	- 22.6	485	7.04	14.34	0.4791	0.5511	616	5 791
18 000	- 20.7	506	7.34	14.94	0.4994	0.5699	619	5 406
17 000	- 18.7	527	7.65	15.57	0.5203	0.5892	621	5 182
16 000	- 16.7	549	7.97	16.22	0.5420	0.6090	624	4 877
15 000	- 14.7	572	8.29	16.89	0.5643	0.6292	626	4 572
14 000	- 12.7	595	8.63	17.58	0.5875	0.6500	628	4 267
13 000	- 10.8	619	8.99	18.29	0.6113	0.6713	631	3 962
12 000	- 8.8	644	9.35	19.03	0.6360	0.6932	633	3 658
11 000	- 6.8	670	9.72	19.79	0.6614	0.7156	636	3 353
10 000	- 4.8	697	10.10	20.58	0.6877	0.7385	638	3 048
9 000	- 2.8	724	10.51	21.39	0.7148	0.7620	640	2 743
8 000	- 0.8	753	10.92	22.22	0.7428	0.7860	643	2 438
7 000	+ 1.1	782	11.34	23.09	0.7716	0.8106	645	2 134
6 000	+ 3.1	812	11.78	23.98	0.8014	0.8359	647	1 829
5 000	+ 5.1	843	12.23	24.90	0.8320	0.8617	650	1 524
4 000	+ 7.1	875	12.69	25.84	0.8637	0.8881	652	1 219
3 000	+ 9.1	908	13.17	26.82	0.8962	0.9151	654	914
2 000	+ 11.0	942	13.67	27.82	0.9298	0.9428	656	610
1 000	+ 13.0	977	14.17	28.86	0.9644	0.9711	659	305
0	+ 15.0	1013	14.70	29.92	1.0000	1.0000	661	0
- 1 000	+ 17.0	1050	15.23	31.02	1.0366	1.0295	664	- 305

Figure 46: Table for pressures and temperatures at different altitudes

B "Appendix 2"

C "Appendix 3"

References

[1] R. W. Gent, N. P. Dart, and J. T. Cansdale, "Aircraft icing," *The Royal Society*, 2000.

[2] M. S. Kirby and R. J. Hansman, "An experimental and theoretical study of the ice accretion process during artificial and natural icing conditions," 1986.

[3] N. W. Service, "Clouds," 2020.

[4] T. J. Vukits and Raytheon, "Overview and risk assessment of icing for transport category aircraft and components," *40th AIAA Aerospace Sciences Meeting & Exhibit*, 2002.

[5] C. Son, S. Oh, and K. Yee, "Quantitative analysis of a two-dimensional ice accretion on airfoils," 2012.

[6] X. Huang, N. Tepylo, V. Pommier-Budinger, M. Budinger, E. Bonaccurso, P. Villedieu, and L. Bennani, "A survey of icephobic coatings and their potential use in a hybrid coating/active ice protection system for aerospace applications," 2019.

[7] M. A. S. Shohag, E. C. Hammel, D. O. Olawale, and O. I. Okoli, "Damage mitigation techniques in wind turbine blades: A review," 2017.

[8] B. Wei., W. Yun., L. H., C. J., Z. G., and S. H. J. M. X. H., "Sdbd based plasma anti-icing: A streamwise plasma heat knife configuration and criteria energy analysis," *International Journal of Heat and Mass Transfer*, 2019.

[9] C. Mayer, "Wind tunnel study of electro-thermal de-icing of wind turbine blades," *International Society of Offshore and Polar Engineers*, 2007.

[10] Y. Yeong, J. Sokhey, and E. Loth, "Ice adhesion on superhydrophobic coatings in anicing wind tunnel, advances in polymer science," 2017.

[11] V. Hejazi, K. Sobolev, and M. Nosonovsky, "From superhydrophobicity to icephobicity: forces and interaction analysis.," 2013.

[12] V. Hejazi, K. Sobolev, and M. Nosonovsky, "From superhydrophobicity to icephobicity: forces and interaction analysis," 2013.

[13] R. Maksel, "What determines an airplane's lifespan?." https://www.airspacemag.com/need-to-know/what-determines-an-airplanes-lifespan-29533465/.

[14] FAA, "Part 25—airworthiness standards: Transport category airplanes," 2020.

[15] FAA, "Part 33—airworthiness standards: Aircraft engines," 2020.

[16] M. Cavcar, "The international standard atmosphere (isa)," 2000.

[17] F. T. Lynch and A. Khodadoust, "Effects of ice accretions on aircraft aerodynamics," *Elsevier Science Ltd*, 2001.

[18] G. Fortin, "Considerations on the use of hydrophobic, superhydrophobic or icephobic coatings as a part of the aircraft ice protection system," *SAE Technical Paper Series*, 2013.

[19] H. W. H. Jeroen E. Dillingh, "Numerical simulation of airfoil ice accretion and thermal anti-icing systems," 2004.

[20] Daniel, Pisquali, S. Breslin, Simon, A. S. Pramod, A. R. Pandie, and B. Shepherd, "Boeing 737 specifi-

cations," Apr 2019.

[21] "Skybrary wiki," Sep 2017.

[22] Federal Aviation Administration, *Aeronautical Information Manual*, Apr 14. TBL 5^{-3-1}.

[23] Y. Cengel and A. Ghajar, *Heat and Mass tranfer Fundamentals and Applications*. McGraw-Hill Education, 2015.

[24] E. Achenbach, "Total and local heat transfer from a smooth circular cylinder in cross-floe at high reynolds number," 1975.

[25] J. Sloan, "787 integrates new composite wing deicing system." https://www.compositesworld.com/articles/787-integrates-new-composite-wing-deicing-system?fbclid=IwAR0mM1Sf$_2$$RZMjggTldVbB0T88z_pF_7UAWGhfRDec0ppXDDW$

[26] "Boeing 787 dreamliner specs." http://www.modernairliners.com/boeing-787-dreamliner/boeing-787-dreamliner-specs/.

[27] "Boeing next-generation 737." https://www.boeing.com/commercial/737ng/.

[28] Skybrary, "Aircraft bleed air systems."

[29] Boeing, "Boeing 787 dreamliner."

[30] D. E. Winterbone, *Advanced Thermodynamics for Engineers (Second Edition)*. Elsevier, 2015.

[31] Y. Lin, H. C. G. Wang, and A. L. 1, "Recent progress in preparation and anti-icing applications of superhydrophobic coatings," 2018.

[32] ICECOAT, "Novel aircraft de-icing concept based on smart coatings with electro-thermal system," 2016.

[33] S. Vallor, "An ethical toolkit for engineering/design practice."

[34] "Colgan air 3407 cvr transcript," april 2020.

[35] C. Biesecker, "Dhs led team demonstrates that commercial aircraft can be remotely hacked," August 2017.

[36] G. Travis, "How the boeing 737 max disaster looks to a software developer," April 2019.

[37] H. Sampson, "What happens when an airline pilot is arrested for drinking on the job?," August 2019.